Modern Plasma Physics Vol. 1

Physical Kinetics of Turbulent Plasmas

P. H. Diamond, S.-I. Itoh and K. Itoh

5

Kinetics of Nonlinear Wave-Wave Interaction

A wave is never found alone, but is mingled with as many other waves as there are uneven places in the object where said wave is produced. At one and the same time there will be moving over the greatest wave of a sea innumerable other waves, proceeding in different directions.

– *Leonardo da Vinci, "Codice Atlantico"*

5.1 Introduction and Overview

5.1.1 Central issues and scope

After our discussions of quasilinear theory and nonlinear wave-particle interaction, it is appropriate to pause, to review where we've been, and to survey where we're going. Stepping back, one can say that the central issues which plasma turbulence theory must address may be classified as:

a) mean field relaxation — how the mean distribution function evolves in the presence of turbulence, and what sort of heating, cross-field

transport, etc. result from that evolution. Though much maligned, mean field theory forms the backbone of most approaches to turbulence. Chapter 3 deals with the most basic approach to the mean field theory of relaxation, namely quasilinear theory—based upon closure using the linear response. Future chapters will discuss more advanced approaches to describing relaxation in a turbulent, collisionless plasma.

b) response — how the distribution function evolves in response to a test perturbation in a turbulent collisionless plasma. Problems of response including nonlinear Landau damping, resonance broadening theory, propagator renormalization, etc are discussed in Chapters 3 and 4, on the kinetics of nonlinear wave-particle interaction.

c) spectra and excitation — how a system of nonlinearly interacting waves or modes couples energy or 'wave quanta density' across a range of space-time scales, given a distribution of forcing, growth and dissipation. In essence, the quest to understand the mechanism of spectral energy transfer and distribution *defines* the "problem of turbulence"—the classic Kolmogorov 1941 (K41) theory of 3D Navier-Stokes turbulence being the most familiar and compelling example. Hence, the discussion of this chapter, now turns to the problem of spectra and excitation.

We approach the problem of spectral transfer dynamics by examining a sequence of illustrative paradigms in wave-wave interaction theory. This sequence begins with coherent wave-wave interactions, proceeds to wave turbulence theory and its methodology, and then addresses simple scaling models of cascades. Future chapters will discuss extensions and related top-

ics, such as closure methods for strong turbulence, methods for the reduction of multi-scale problems, disparate scale interactions, etc. The list of familiar examples discussed includes, but is not limited to:

→ resonant wave interactions
→ wave kinetics
→ decay and modulational processes
→ scaling theory of turbulent cascade

Familiar conceptual issues encountered along the way include:

→ the implication of conservation laws for transfer processes
→ basic time scale orderings and their relevance to the unavoidable (yet unjustifiable!) *assumption* of the applicability of statistical methods
→ restrictions on the wave kinetic equation
→ the type of interactions and couplings (i.e. local and non-local) possible. Anticipating subsequent discussions of structure formation, we give special attention to *non-local* wave-wave interactions.
→ spectral structure and its sensitivity to the distribution of sources and sinks.

Both lists are long and together leave no doubt that the subject of wave-wave interaction is a vast and formidable one!

5.1.2 Hierarchical progression in discussion

Given the scope of the challenge, we structure our discussion as a hierarchical progression through three sections. These are:

a) the integrable dynamics of three coupled modes

These simple, "toy model" studies reveal the basic elements of the

dynamics of mode-mode interactions (such as the Manley-Rowe relations) and illustrate the crucial constraints which conservation laws impose on the nonlinear transfer processes. Though simple, these models constitute the essential foundation of the theory of wave-wave interaction. One appealing feature of these basic paradigms is that their dynamics can be described using easily visualizable geometrical constructions, familiar from classical mechanics.

b) the physical kinetics of multi-wave interactions and wave turbulence

The culmination of this discussion is the derivation of a wave-kinetic equation, similar to the Boltzmann equation, for the exciton or wave population density $N(\boldsymbol{k}, \omega_{\boldsymbol{k}}, t)$ and its evolution. The wave population density $N(\boldsymbol{x}, \boldsymbol{k}, t)$ may be thought of as a distribution function for quasi-particles in the phase space $(\boldsymbol{x}, \boldsymbol{k})$. Thus, wave population dynamics resembles quasi-particle dynamics. Like the Boltzmann equation for particles, the wave kinetic equation is *fundamentally statistical*, rests on assumptions of weak correlation and microscopic chaos, and takes the generic form:

$$\frac{\partial N}{\partial t} + (\boldsymbol{v}_{\mathrm{gr}} + \boldsymbol{v}) \cdot \boldsymbol{\nabla} N - \frac{\partial}{\partial \boldsymbol{x}} (\omega + \boldsymbol{k} \cdot \boldsymbol{v}) \cdot \frac{\partial N}{\partial \boldsymbol{k}} = C(N)$$

$$C(N) = \sum_{\substack{\boldsymbol{k}', \boldsymbol{k}'' \\ \boldsymbol{k}' + \boldsymbol{k}'' = \boldsymbol{k}}} \delta(\omega_{\boldsymbol{k}} - \omega_{\boldsymbol{k}'} - \omega_{\boldsymbol{k}''}) \times \left\{ C_{\mathrm{s}}\left(\boldsymbol{k}', \boldsymbol{k}''\right) N_{\boldsymbol{k}'} N_{\boldsymbol{k}''} - C_{\mathrm{s}}\left(\boldsymbol{k}', \boldsymbol{k}\right) N_{\boldsymbol{k}'} N_{\boldsymbol{k}} \right\}.$$

Wave kinetics first appeared in the theory of the statistical mechanics of lattice vibrational modes—i.e. as in the Einstein and Debye theory of solids, etc. We emphasize, though, that those early applications

were concerned with systems of thermal fluctuations *near* equilibrium, while wave turbulence deals with strongly excited systems *far* from equilibrium. One quantity which distinguishes 'equilibrium' from 'non-equilibrium' solutions of the wave-kinetic equation is the exciton density flux in $\boldsymbol{k}$, i.e.

—near equilibrium, the flux of exciton density (i.e. energy) from mode to mode is weak, so the spectrum is determined by a scale-by-scale balance of emission and absorption, consistent with the fluctuation-dissipation theorem (Fig. 2.1)

—far from equilibrium the scale-to-scale flux (which can be either local or non-local in $\boldsymbol{k}$!) dominates local emission and absorption, as in the inertial rage cascade in fluid turbulence. The spectrum is determined by the condition of flux stationarity, which entails the solution of a differential equation with appropriate boundary conditions.

The wave kinetic equation can either be solved to obtain the spectrum or can be integrated to derive (moment) equations for net wave energy and momentum density. The latter may be used to calculate macroscopic consequences of wave interaction, such as wave-induced stresses and wave energy flux, by analogy with the theory of radiation hydrodynamics.

c) the scaling theory of cascades in wave turbulence.

The classic example of a cascade scaling theory is the K41 model of Navier-Stokes turbulence. Though they may appear simple, or even crude, to a casual observer, scaling theories can be subtle and frequently are the only viable approach to problems of wave turbulence.

Scaling theories and wave kinetics are often used synergistically when approaching complex problems in wave turbulence.

d) non-local interaction in wave turbulence.

Wave turbulence can transfer energy both locally (i.e. between modes with neighboring $\boldsymbol{k}$'s) and non-locally (i.e. between modes of very different scale). In this respect, wave turbulence is much richer and more complex than high R_e fluid turbulence (as usually thought of), despite the fact that wave turbulence is usually weaker, with a lower 'effective Reynolds number'. Non-local interaction is important to the dynamics of structure formation, as a possible origin of intermittency in wave turbulence, and as an energy flow channel which cannot be ignored.

Note that as we progress through the sequence of sections a) → b) → c), the level of rigor with which we treat the dynamics degrades, in return for access to a broader regime of applicability—i.e. to systems with more degrees of freedom or higher wave intensity levels. Thus, in a), the analysis is *exact* but restricted to resonant interaction of only three modes. In b), the description is statistical and cast in terms of a Boltzmann-like wave kinetic equation. As for the Boltzmann equation in the kinetic theory of gases (KTG) (Chapman and Cowling, 1952), wave kinetics rests upon assumptions of weak interaction (akin to weak correlations in KTG) and microscopic chaos—i.e. the Random Phase Approximation (akin to the Principle of Molecular Chaos in KTG). However, wave kinetics *does* capture anisotropy and scale dependency in the coupling coefficients and in the selection rules which arise from the need for resonant matching of frequencies. In contrast to the toy models discussed in a), the wave kinetics of b) can describe the

evolution of broad spectra with many interacting waves, though this gain comes with the loss of all phase information. However, wave kinetics cannot address wave breaking (i.e. fluctuation levels at or beyond the mixing length level) or other instances where nonlinear rates exceed linear wave frequencies. A systematic treatment of breaking, wave resonance broadening and other strongly nonlinear stochastic phenomena requires the use of renormalized closure theory, which is the subject of Chapter 6. At the crudest level, as discussed in c), one can proceed in the spirit of the Kolmogorov and Richardson model of the energy cascade in Navier-Stokes turbulence and construct scaling theories for spectral evolution. Scaling models, which are basically zero-D, constitute one further step along the path of simplification, in that they release *all* phase and memory constraints in return for ease of applicability to systems with greater complexity. In scaling models, scale-dependent couplings are represented by simple multiplicative factors, anisotropy is often (though not always) ignored and spectral transfer is assumed to be local in scale. Nevertheless, scaling arguments are often the only tractable way to deal with problems of strong wave turbulence, and so merit discussion in this chapter.

5.2 The Integrable Dynamics of Three Coupled Modes

"When shall we three meet again?"
– *Shakespeare, "Macbeth"*

In this section, we discuss the simple and fundamental paradigm of three resonantly coupled waves. This discussion forms the foundation for much of our later treatment of wave kinetics and so is of some considerable importance.

5.2.1 Free asymmetric top (FAT)

Surely the *simplest* example of a system with three resonantly coupled degrees of freedom is the free asymmetric top (FAT), familiar from elementary mechanics (Landau and Lifshitz, 1976). The FAT satisfies Euler's equation

$$\frac{\mathrm{d}\boldsymbol{L}}{\mathrm{d}t} + \boldsymbol{\Omega} \times \boldsymbol{L} = 0, \tag{5.1a}$$

which may be written component-by-component as

$$\frac{\mathrm{d}\Omega_1}{\mathrm{d}t} + \left(\frac{I_3 - I_2}{I_1}\right)\Omega_2\Omega_3 = 0, \tag{5.1b}$$

$$\frac{\mathrm{d}\Omega_2}{\mathrm{d}t} + \left(\frac{I_1 - I_3}{I_2}\right)\Omega_3\Omega_1 = 0, \tag{5.1c}$$

$$\frac{\mathrm{d}\Omega_3}{\mathrm{d}t} + \left(\frac{I_2 - I_1}{I_3}\right)\Omega_1\Omega_2 = 0. \tag{5.1d}$$

Here the three components of the angular momentum $\boldsymbol{\Omega}$ may be thought of as analogous to evolving coupled mode amplitudes. The inertia tensor is diagonal, with principal axes 1, 2, 3 and $I_3 > I_2 > I_1$. Of course $\boldsymbol{L} = \boldsymbol{I} \cdot \boldsymbol{\Omega}$ where $\boldsymbol{I}$ is the moment of inertia. Equation (5.1) can be solved straightforwardly in terms of elliptic functions, but it is far more illuminating to 'solve' the FAT geometrically, via the elegant Poinsot construction. The essence of the Poinsot construction exploits the fact that, the FAT has *two* quadratic integrals of the motion, namely $L^2 = \boldsymbol{L} \cdot \boldsymbol{L}$—the magnitude of the angular momentum vector, and the energy. These invariants follow from Euler's equation. Thus, since

$$L^2 = L_1^2 + L_2^2 + L_3^2 = L_0^2, \tag{5.2a}$$

$$E = \frac{L_1^2}{2I_1} + \frac{L_2^2}{2I_2} + \frac{L_3^2}{2I_3} = E_0, \tag{5.2b}$$

$\boldsymbol{L}(t) = \boldsymbol{I} \cdot \boldsymbol{\Omega}(t)$ is *simultaneously* constrained to evolve on:

i) the surface of a sphere of constant radius L_0

ii) the surface of ellipsoid, with semi-majour axes of length $(2E_0 I_{1,2,3})^{1/2}$

The set of curves which trace out the possible intersections of the sphere and ellipsoid also trace the possible trajectories of FAT motion. This construction constitutes the Poinsot construction, and is shown in Fig. 5.1.

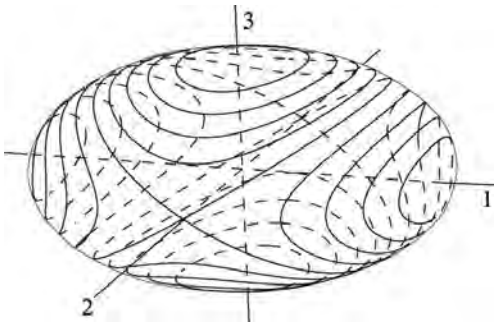

Fig. 5.1. Poinsot constructing for the Free Asymmetric Top. Note that trajectories originating at the poles of the "2" axis encircle the ellipsoid.

Several features of the FAT motion can be deduced simply by inspection of the Poinsot construction. First, all trajectories are *closed*, so the dynamics are *reversible*. There is *no* intrinsic tendency for energy to accumulate in any one degree of freedom. Second, trajectories originating near the "1" or "3" axes (corresponding to I_1 or I_3) are closed and *localized* to the vicinity of those axes, while trajectories initialized near the "2" axis wrap around the body of the ellipsoid, and so are *not localized*. Thus, an initial condition starting near the "2" axis is linearly unstable, as is well known from rigid body stability theory. However, the fact that all trajectories are closed tells us that the linear solution breaks down as instability grows and then saturates, and $\boldsymbol{L}$ ultimately returns to its point of origin.

5.2.2 Geometrical construction of three coupled modes

Interestingly, a similar geometrical construction which captures the essential dynamics of resonant 3-mode coupling may be derived from the resonant mode coupling equations and their conservation properties. Most generally, resonant coupling dynamics arises in the perturbative solution to the interaction of three nonlinearly coupled harmonic oscillators, with Hamiltonian

$$H = \sum_i \left(\frac{p_i^2}{2m} + \frac{\omega_i^2 q_i^2}{2} + 2V q_1 q_2 q_3 \right) \tag{5.3a}$$

and Hamiltonian equations of motion (EOM)

$$\dot{p}_i = -\partial H/\partial q_i, \quad \dot{q}_i = \partial H/\partial p_i, \tag{5.3b}$$

so the coupled oscillator EOMs are

$$\ddot{q}_i + \omega_i^2 q_i = 2V q_j q_k. \tag{5.3c}$$

The essence of the perturbative, *weak coupling* approximation applied here is to restrict amplitudes to the limit where nonlinearity is small relative to the wave frequency (i.e. $\left|Vq \ll \omega^2\right|$), so the time for nonlinear energy transfer is slower than a wave oscillation time. Thus,

$$q_i(t) = a_i(t)\, e^{-i\omega_i t} + a_i^*(t)\, e^{i\omega_i t} \tag{5.4}$$

where the time variation of the phase factor $\exp(\pm i\omega_i t)$ accounts for the fast oscillation frequency and that of the amplitude $a_i(t)$ accounts for slow variation due to nonlinear interaction. The basic ordering is $|\dot{a}_i/a| \ll \omega_i$. Substitution of Eq. (5.4) into Eq. (5.3c) (for $i = 1$) then yields, after some

rearrangement:

$$\frac{\mathrm{d}^2 a_1}{\mathrm{d}t^2} - 2i\omega_1 \frac{\mathrm{d}a_1(t)}{\mathrm{d}t} = e^{2i\omega_1 t}\left(\frac{\mathrm{d}^2 a_1^*}{\mathrm{d}t^2} + 2i\omega_1 \frac{\mathrm{d}a_1^*}{\mathrm{d}t}\right) - 2V\Big(a_2 a_3 \exp\left[i\left(\omega_1 - \omega_2 - \omega_3\right)t\right] + a_2 a_3^* \exp\left[i\left(\omega_1 - \omega_2 + \omega_3\right)t\right] + a_2^* a_3 \exp\left[i\left(\omega_1 + \omega_2 - \omega_3\right)t\right] + a_2^* a_3^* \exp\left[i\left(\omega_1 + \omega_2 + \omega_3\right)t\right]\Big). \quad (5.5)$$

Since the question of concern here is the nature of energy transfer among oscillators on time scales *long* compared to the wave period $2\pi/\omega_1$, we aim to describe secular evolution of $a_1(t)$, which can occur only if the RHS of Eq. (5.5) does *not* oscillate rapidly in time. Hence, we arrive at the *resonance* or *frequency matching condition* or '*selection rule*' which is:

$$\omega_1 \pm \omega_2 \pm \omega_3 = 0. \quad (5.6)$$

Satisfying this 3-wave resonance condition ensures the secular drive of each mode by the other two. Proceeding without loss of generality by taking $\omega_3 = \omega_1 + \omega_2$, we obtain

$$i\omega_1 \frac{\mathrm{d}a_1(t)}{\mathrm{d}t} = V a_2^* a_3 + \text{oscillatory terms},$$

which for weak interaction as $t \to \infty$ reduces to

$$i\omega_1 \frac{\mathrm{d}a_1(t)}{\mathrm{d}t} = V a_2^* a_3. \quad (5.7)$$

Implementing similar expansions for $i = 2, 3$ yields the *resonant 3-wave coupling equations*

$$i\omega_1 \frac{\mathrm{d}a_1(t)}{\mathrm{d}t} = V a_2^*(t)\, a_3(t), \quad (5.8a)$$

$$i\omega_2 \frac{\mathrm{d}a_2(t)}{\mathrm{d}t} = V a_1^*(t)\, a_3(t), \quad (5.8b)$$

$$i\omega_3 \frac{\mathrm{d}a_3(t)}{\mathrm{d}t} = V a_1(t)\, a_2(t). \quad (5.8c)$$

In general, the coupling coefficient V may be complex and may depend on the parameters of waves 1, 2, 3. For example, the resonant coupling equations for three interacting Rossby waves (as given by Pedlosky (Pedlosky, 1987), after Longuet-Higgins and Gill (Longuet-Higgins et al., 1967)) are:

$$\begin{aligned}
&\frac{\mathrm{d}a_1}{\mathrm{d}t} + \frac{B\left(\boldsymbol{k}_2, \boldsymbol{k}_3\right)}{k_1^2 + F} a_2 a_3 = 0, \\
&\frac{\mathrm{d}a_2}{\mathrm{d}t} + \frac{B\left(\boldsymbol{k}_3, \boldsymbol{k}_1\right)}{k_2^2 + F} a_3 a_1 = 0, \\
&\frac{\mathrm{d}a_3}{\mathrm{d}t} + \frac{B\left(\boldsymbol{k}_1, \boldsymbol{k}_2\right)}{k_3^2 + F} a_1 a_2 = 0.
\end{aligned} \tag{5.9a}$$

See Appendix for explanation of the equations for Rossby waves. Here the coupling coefficient is

$$B\left(\boldsymbol{k}_m, \boldsymbol{k}_n\right) = \frac{1}{2}\left(k_m^2 - k_n^2\right)\left(\boldsymbol{k}_m \times \boldsymbol{k}_n \cdot \hat{z}\right). \tag{5.9b}$$

The parameter F indicates the scale length that dictates the wave dispersion, and the resonance conditions are

$$\begin{aligned}
&\omega_{mn} \pm \omega_m \pm \omega_n = 0, \\
&\boldsymbol{k}_{mn} \pm \boldsymbol{k}_m \pm \boldsymbol{k}_n = 0.
\end{aligned} \tag{5.9c}$$

Certainly, the resonant coupling equations for model amplitudes $a_1(t)$, $a_2(t)$, $a_3(t)$ bare a close resemblance to the Euler equations for $\Omega_1(t)$, $\Omega_2(t)$, $\Omega_3(t)$ in the FAT. Analogy with the top suggests we should immediately identify the integrals of the motion (IOM's) for the resonant coupling equations. It is no surprise that one quantity conserved by Eq. (5.8) is the total energy of the system, i.e.

$$E = \frac{1}{2}\omega_1^2 \left|a_1(t)\right|^2 + \frac{1}{2}\omega_2^2 \left|a_2(t)\right|^2 + \frac{1}{2}\omega_3^2 \left|a_3(t)\right|^2, \tag{5.10}$$

which is also derived from Eq. (5.8) by noting the relation $\omega_3 = \omega_1 + \omega_2$

Conservation of energy, i.e. $\mathrm{d}E/\mathrm{d}t = 0$, is demonstrated straightforwardly using Eqs. (5.8a)-(5.8c), their complex conjugates, and the resonance condition $\omega_3 - \omega_1 - \omega_2 = 0$. A (somewhat) less obvious conservation relation may be derived from the mode amplitude equations (Eq. (5.8)) by observing

$$\begin{aligned} \frac{\mathrm{d}}{\mathrm{d}t}\left(\omega_1 \left|a_1\right|^2\right) &= \frac{\mathrm{d}}{\mathrm{d}t}\left(\frac{\omega_1^2 \left|a_1^2\right|}{\omega_1}\right) = V \,\mathrm{Re}\left(-i a_1^* a_2^* a_3\right) \\ &= V \,\mathrm{Im}\left(a_1^* a_2^* a_3\right), \end{aligned} \tag{5.11a}$$

and similarly

$$\frac{\mathrm{d}}{\mathrm{d}t}\left(\frac{\omega_2^2 \left|a_2\right|^2}{\omega_2}\right) = V \,\mathrm{Im}\left(a_1^* a_2^* a_3\right), \tag{5.11b}$$

$$\begin{aligned} \frac{\mathrm{d}}{\mathrm{d}t}\left(\frac{\omega_3^2 \left|a_3\right|^2}{\omega_3}\right) &= V \,\mathrm{Im}\left(a_3^* a_1 a_2\right) \\ &= -V \mathrm{Im}\left(a_1^* a_2^* a_3\right), \end{aligned} \tag{5.11c}$$

since $\mathrm{Im}\ a^* = -\mathrm{Im}\ a$. Taken together, Eqs. (5.11a), (5.11b), (5.11c) state that

$$\frac{\mathrm{d}}{\mathrm{d}t}\left(E_1/\omega_1\right) = \frac{\mathrm{d}}{\mathrm{d}t}\left(E_2/\omega_2\right) = -\frac{\mathrm{d}}{\mathrm{d}t}\left(E_3/\omega_3\right), \tag{5.12}$$

where $E_j = \omega_j^2 \left|a_j\right|^2$ $(j = 1, 2, 3)$. We remind the reader that here, the selection or frequency match rule is $\omega_3 = \omega_2 + \omega_1$. That is, ω_3 is the highest frequency.

5.2.3 Manley-Rowe relation

Equations (5.11) and (5.12) form a geometrical construction for three (resonantly) coupled modes. Equation (5.12) is a particular statement of an important and general identity called the Manley-Rowe relation. This relation is best understand by observing that E_i/ω_i has dimension of action

(i.e. energy $*$ time) and so may be thought of as a *mode action*

$$N_i = E_i/\omega_i, \qquad E_i = N_i\omega_i$$

also reminds us of the familiar semi-classical formula $E = N\omega$, which relates N, the number of quanta, to the energy E and frequency ω (for $N \gg 1$). Hence N may also be usefully thought of as the 'number' of wave quanta. The significance of the Manley-Rowe relation then emerges as an input-out balance for wave quanta! Specifically, the Manley-Rowe relation (M-R relation) which (most generally) requires that if

$$\omega_{k_\alpha} + \omega_{k_\beta} = \omega_{k_\gamma}, \tag{5.13a}$$

then

$$\frac{\mathrm{d}N\,(k_\alpha)}{\mathrm{d}t} = \frac{\mathrm{d}N\,(k_\beta)}{\mathrm{d}t} = -\frac{\mathrm{d}N\,(k_\gamma)}{\mathrm{d}t}, \tag{5.13b}$$

effectively states that should modes α, β beat together to drive mode γ, then for every exciton or wave 'created' in modes γ, one quantum *each* must be lost from modes α, β. The M-R relation is also reversible, so that if instead one quantum of mode γ is destroyed, then one quantum each for modes α, β must then be created as a result of the interaction process. The M-R relation is depicted graphically in Fig. 5.2. The M-R

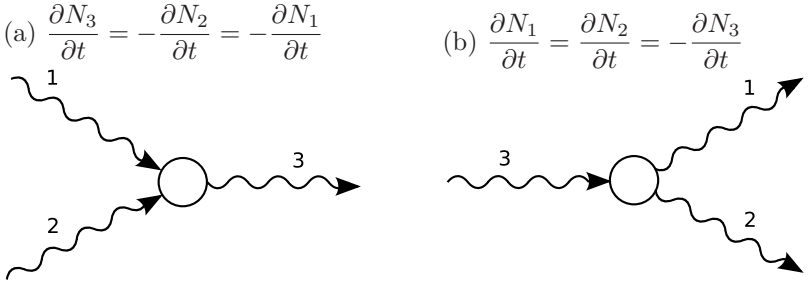

Fig. 5.2. Equivalent statements of the Manley-Rowe relations for three interacting waves.

relation has interesting implications for the often relevant limit where one mode has frequency much lower than the other two, i.e. $\omega_1 + \omega_2 = \omega_3$ but $\omega_1 \ll \omega_2, \omega_3$. Such instances of slow modulation are relevant to problems of drift wave-zonal flow interaction, Langmuir turbulence and other important applications involving structure formation, which is discussed in Chapter 6. In this case, where $\omega_2 \cong \omega_3$, the behavior of modes 2 and 3 must be virtually identical, but the M-R relation forces $\mathrm{d}N_2/\mathrm{d}t = -\mathrm{d}N_3/\mathrm{d}t$!? This paradox is resolved by requiring

$$\frac{\mathrm{d}N_2}{\mathrm{d}t} = \frac{\mathrm{d}N_3}{\mathrm{d}t} = 0,$$

so that the number of quanta N is conserved in the interaction (i.e. $\mathrm{d}N/\mathrm{d}t = 0$). Thus, *in the case where one mode is a slow modulator of the other two, the Manley-Rowe relation is equivalent to the statement of adiabatic invariance of the wave quanta population.* This is sketched in Figure 5.3.

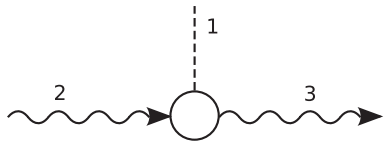

Fig. 5.3. For slow modulation by mode 1, Manley-Rowe relation implies adiabatic invariance of quanta populations.

Taken together, then, energy conservation and the M-R relations, i.e.

$$E_0 = \left(\omega_1^2 a_1^2 + \omega_2^2 a_2^2 + \omega_3^2 a_3^2\right) \tag{5.14}$$

and

$$\omega_1 a_1^2 + \omega_3 a_3^2 = N_1\left(0\right) + N_3\left(0\right) \tag{5.15a}$$

or equivalently

$$\omega_2 a_2^2 + \omega_3 a_3^2 = N_2(0) + N_3(0) \tag{5.15b}$$

specify *two* constraints on the interacting mode amplitudes in a resonant tried. Here, the number of quanta of mode i, $N_{\mathrm{i}}(0)$, refers to the initial quanta number of mode i, and so, $E_0 = \omega_1 N_1(0) + \omega_2 N_2(0) + \omega_3 N_3(0)$. Consideration of Eqs. (5.14), (5.15b) reveals that the system's trajectories in the phase space $\left(\sqrt{\omega_1}a_1, \sqrt{\omega_2}a_2, \sqrt{\omega_3}a_3\right)$ are given by the curves of intersection between:

— the ellipsoid of constant energy, with semi-majour axes $(E_0/\omega_1)^{1/2}$, $(E_0/\omega_2)^{1/2}$, $(E_0/\omega_3)^{1/2}$ and

— Manley-Rowe cylinders, oriented parallel to the a_1 and a_2 axes, with radii $(N_2(0) + N_3(0))^{1/2}$, $(N_1(0) + N_3(0))^{1/2}$.

This construction clearly resembles, but is subtlely different from, the Poinsot construction for the FAT trajectories. From Fig. 5.4, we can immediately see that:

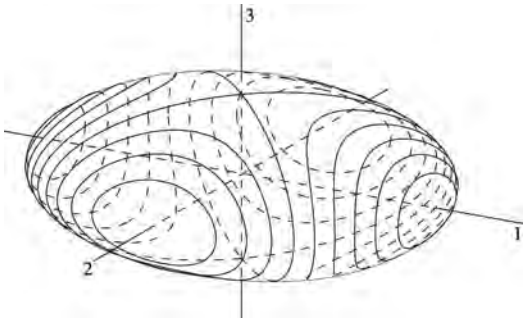

Fig. 5.4. Poinsot construction for three interacting modes. Note that trajectories originating at the "3" axis encircle the ellipsoid.

→ as for the FAT, all trajectories are closed curves, so all *motion is reversible and periodic*

but,

— since $\omega_3 > \omega_2 > \omega_1$, the intersections of the Manley-Rowe cylinders and the energy ellipsoid always encircle the ellipsoid if $N_3(0) \gg N_2(0), N_1(0)$, while trajectories with initial conditions for which $N_2(0) \gg N_1(0), N_3(0)$ remain localized near the poles at the a_2 or a_1 axes.

5.2.4 Decay instability

This tells us that the *highest* frequency mode is subject to *decay instability* if it is initialized with the largest population or externally driven. Recall for contrast that in the FAT, decay instability occurred for initialization near the Ω_2 axis, i.e. which corresponds to the mode with intermediate moment of inertia ($I_3 > I_2 > I_1$). In both cases, however, the nonlinear motion is periodic and all trajectories close on themselves.

The prediction of decay instability may be verified by linearizing Eqs. (5.8a)-(5.8c) about the state $a_3(t) \cong a_0$, $a_{1,2}(t) = \delta a_{1,2} \ll a_0$. This gives

$$i\omega_1 \frac{\mathrm{d}\delta a_1}{\mathrm{d}t} = V\delta a_2^* a_0 \tag{5.16a}$$

$$i\omega_2 \frac{\mathrm{d}\delta a_2}{\mathrm{d}t} = V\delta a_1^* a_0 \tag{5.16b}$$

$$i\omega_3 \frac{\mathrm{d}a_3}{\mathrm{d}t} = V\delta a_1 \delta a_2 \simeq 0, \tag{5.16c}$$

so

$$\omega_1\omega_2 \frac{\mathrm{d}^2}{\mathrm{d}t^2}\delta a_1 = |Va_0|^2 \delta a_1, \tag{5.17}$$

and the decay instability growth rate is given by the energy exchange rate

$$\gamma_E^2 = |V|^2 |a_0|^2 / \omega_1 \omega_2. \tag{5.18}$$

Here, we took $\omega_1, \omega_2 > 0$, with $\omega_3 = \omega_1 + \omega_2$. It is easy to verify that should the pump be a mode other that the one with the highest frequency, then the decay process is stable. The time evolutions for decay unstable and decay stable processes are shown in Fig. 5.4. If initial state is very close to the X-point (i.e., the intersection with the third axis), the trajectory deviates from the X-point, and the energy of the mode-3 is converted to those of mode-1 and mode-2. In contrast, if the initial state is close to the O-point (e.g., the intersection with the 2nd axis), the trajectory encircles the O-point, and the deviation does not grow. Observe that the important limit of the *parametric subharmonic instability*, with $\omega_1 \sim \omega_2$ and $\omega_3 \sim 2\omega_1$, is a particular case of the decay instability described here. (See (Mima and Nishikawa, 1984) for detailed explanation of parametric instabilities.)

The decay instability growth rate γ_E is a fundamental time scale. Equation (5.18) sets the rate of coherent energy transfer out of a strongly populated or 'pumped' mode. The rate γ_E is one of a few characteristic rates, the ordering of which determines which theoretical description is appropriate for the system under study. For example, whether a coherent or stochastic mode coupling approach is relevant depends on the relative size of the spectral auto-correlation (self-coherence) rate and the decay instability rate of Eq. (5.16). This comparison is discussed further in the next section.

5.2.5 Example—drift-Rossby waves

As drift-Rossby waves and drift wave turbulence are critically important to this discussion of plasma turbulence and self-organization, the problem

of three interacting drift-Rossby waves merits special discussion here. The alert reader may already have noted that Eqs. (5.9a)— the mode amplitude equations for three interacting Rossby waves—don't have quite the same structure as Eqs. (5.8)—the usual, generic amplitude equations for three coupled nonlinear oscillators, and that no analogue of Eq. (5.12) is apparent. However, given that the Hasegawa-Mima or quasi-geostrophic equation (Hasegawa and Mima, 1978) conserves *both* energy and potential enstrophy (see Appendix 1), it is evident that Eq. (5.9a) must also conserve these, so we can simply state that

$$E_0 = \sum_i \left(k_i^2 + F\right) a_i^2/2 \tag{5.19a}$$

and

$$\Omega_0 = \sum_i \left(k_i^2 + F\right)^2 a_i^2/2 \tag{5.19b}$$

are both integral of motions (IOMs). Interestingly, the structure of these IOMs—and, more generally, the structure of the problem of 3-mode interaction for drift waves—are virtually *identical* to their counterparts for the FAT. Thus, the correspondence rules

$$\begin{gathered} \left(k_i^2 + F\right) a_i^2 \to L_i^2 \\ \left(k_i^2 + F\right) \to 1/I_i \end{gathered} \tag{5.20}$$

effectively map the problem of 3 interacting drift-Rossby waves to the familiar example of the FAT. This isomorphism enables us to again utilize geometrical intuition gained from experience with the Poinsot construction. To this end, we can immediately note that

— the ordering of moments of inertia $I_1 < I_2 < I_3$ maps to the wave number ordering $k_1^2 > k_2^2 > k_3^2$

— then for three interacting drift-Rossby waves, the correspondence to Fig. 5.1 indicates that the wave with the *intermediate* value of k^2 (i.e. k_2) should be unstable to decay, if it is strongly excited.

— this expectation is supported by a "calculation by correspondence", i.e. since for the FAT

$$\gamma_{\text{decay}}^2 = \left(\frac{(I_3 - I_2)(I_2 - I_1)}{I_1 I_3} \right) \Omega_2^2(0), \tag{5.21}$$

so using the correspondence 'rules' gives

$$\rightarrow \frac{\left[\left(\frac{1}{(k_3^2+F)} - \frac{1}{(k_2^2+F)} \right) \left(\frac{1}{(k_2^2+F)} - \frac{1}{(k_1^2+F)} \right) \right] A_0^2}{\left(1/\left(k_1^2+F\right)\right)\left(1/\left(k_3^2+F\right)\right)}$$

so

$$\gamma_{\text{decay}}^2 \sim \frac{\left(k_2^2 - k_3^2\right)\left(k_1^2 - k_2^2\right)}{\left(k_2^2+F\right)^2} A_0^2. \tag{5.22}$$

Here $A_0^2 \sim a_2(0)^2$. This calculation by correspondence confirms our expectations that the intermediate wave number mode is the one which can be decay unstable. These results may also be obtained from a straightforward linear analysis of Eqs. (5.9).

— again, the three wave interaction dynamics is intrinsically *periodic* and *reversible*. There is no apriori tendency for energy to accumulate in any single mode.

Two comments are in order here. First, the decay instability of the intermediate wave number mode pumps both the shorter and longer wave length modes, and so may be thought of as a "dual decay process". This has sometimes been invoked as a harbinger of the familiar dual cascade of 2D turbulence. Though both the dual decay and dual cascade have their

origins in the simultaneous conservation of energy and enstrophy, the direct relevance of dual decay to dual cascade is dubious since:

— the decay process is one of resonant 3 wave coupling—i.e. frequency match is required.
— the 3-wave interaction process is time reversible, while the cascade is not.

Second, care must be taken to recognize that the decay of intermediate wave number does not translate trivially to frequency. Since $\omega_k = k_y V_{\mathrm{de}} / \left(F + k^2\right)$, where V_{de} is the diamagnetic velocity of electrons for drift waves, the decay instability criterion

$$\left(k_3^2 - k_2^2\right)\left(k_2^2 - k_1^2\right) > 0 \tag{5.23a}$$

can be re-expressed as

$$\left(\frac{k_{y2}}{\omega_2} - \frac{k_{y1}}{\omega_1}\right)\left(\frac{k_{y3}}{\omega_3} - \frac{k_{y2}}{\omega_2}\right) > 0. \tag{5.23b}$$

This implies that

$$\frac{\left(\omega_3 k_{y2} - \omega_2 k_{y3}\right)^2}{\omega_1 \omega_3 \omega_2^2} > 0 \tag{5.24}$$

for instability. Hence, instability requires $\omega_1 \omega_3 > 0$, but the triad resonance condition also requires $\omega_2 = -\left(\omega_1 + \omega_3\right)$. These two requirements are reconcilable *only* if the unstable wave has the *highest frequency* in the triad. Thus, we see that in the resonant interaction of drift-Rossby waves, the *highest frequency* wave is the unstable one. Note that the resemblance of this result to that of Eq. (5.18) is somewhat coincidental. Here, an explicit form of the drift wave dispersion relation was used to relate $\boldsymbol{k}$ to $\omega_{\boldsymbol{k}}$, while in the discussion leading up to Eq. (5.18), we considered generic nonlinear oscillators.

5.2.6 Example—unstable modes in a family of drift waves

Another illustrative example of the three coupled mode is constructed for unstable modes in a family of drift waves. Analysis of the ion-temperature-gradient mode (ITG mode (Rudakov and Sagdeev, 1960; Coppi et al., 1967; Mikailowski, 1992; Horton, 1999; Weiland, 2000)) instability is briefly shown here following the discussion in (Lee and Tang, 1988; Parker et al., 1994; Watanabe et al., 2000).

A simple inhomogeneous plasma slab is chosen (main magnetic field is in the z-direction, and the density and ion temperature have gradients in the x-direction, the scale lengths of gradients of them are given by L_n and L_{T_i}, respectively). Unstable waves propagate in the direction of the diamagnetic drift (y-direction). In order to construct a three-mode model, one unstable mode with $(k_x, k_y) = (\pm k, \pm k)$ is kept, which has a linear growth rate γ_{L}, and the second harmonics with $(k_x.k_y) = (\pm 2k, 0)$, which works for the nonlinear stabilization of the linearly unstable mode, is taken into account as well. The wave number component in the direction of the magnetic field is given by $k_z = \theta \rho_i L_n^{-1} k_y$, where θ is a fixed parameter here. The Vlasov equation, which is truncated at these two components, takes a form

$$\left(\frac{\partial}{\partial t} + ik\theta v\right) f_{1,1} + 2ik^2\phi \mathrm{Im}\, f_{2,0} = -ik\phi \left(1 + \frac{2L_n}{L_{T_i}}\left(v^2 - 1\right) + \theta v\right) F_{\mathrm{M}}, \tag{5.25a}$$

$$\frac{\partial}{\partial t}\mathrm{Im}\, f_{2,0} = 4k^2 \mathrm{Im}\left(\phi f_{1,1}\right), \tag{5.25b}$$

where ϕ is the normalized electrostatic potential perturbation for the unstable mode, v is the parallel velocity, F_{M} is the local Maxwellian distribution, the suffix $1,1$ and $2,0$ denote unstable and stable modes, respectively, and length and velocity are normalized to the ion gyroradius ρ_i and ion thermal

velocity, respectively. In the linear response, the growth rate is determined by the eigenvalue equation $\int \mathrm{d}v\, f_{1,1} = \phi$

$$\int \mathrm{d}v\, \frac{1 + 2L_n L_{T_i}^{-1}\left(v^2 - 1\right) + \theta v}{\omega - k\theta v + i\gamma_{\mathrm{L}}} k F_{\mathrm{M}} = 1.$$

When the gradient ratio $L_n L_{T_i}^{-1}$ is large, strong instability is possible to occur.

The eigenfunction of the linearly unstable mode for the perturbed distribution function, $f_{\mathrm{L}}(v) = f_{\mathrm{L,\,r}}(v) + i f_{\mathrm{L,\,i}}(v)$, is employed and the perturbed distribution function of the unstable mode is set as

$$f_{1,1}(v,t) = \left\{a(t)\, f_{\mathrm{L,\,r}}(v) + i b(t)\, f_{\mathrm{L,\,i}}(v)\right\} \exp\left(-i\omega t\right), \tag{5.26a}$$

where ω is the real frequency, and $a(t)$ and $b(t)$ indicate the amplitude. The imaginary part of the second harmonics has the same functional form as $f_{\mathrm{L,\,i}}(v)$, and

$$\mathrm{Im}\, f_{2,0}(v,t) = c(t)\, f_{\mathrm{L,\,i}}(v). \tag{5.26b}$$

Substituting Eq. (5.26) into Eq. (5.25), with the help of charge neutrality condition, $\phi(t) = \int \mathrm{d}v\, f_{1,1}(v,t)$, a set of coupled equations for amplitudes (a, b, c) is obtained as

$$\frac{\mathrm{d}}{\mathrm{d}t} a = \gamma_{\mathrm{L}} b, \tag{5.27a}$$

$$\frac{\mathrm{d}}{\mathrm{d}t} b = \gamma_{\mathrm{L}} a - 2k^2 ac, \tag{5.27b}$$

$$\frac{\mathrm{d}}{\mathrm{d}t} c = 4k^2 ac. \tag{5.27c}$$

The nonlinear coupling terms are quadratic, although not identical to those in Eq. (5.8).

This set of equations shows an exponential growth when the amplitude is

small, $a, b, c \to 0$. In addition, this set has two types of stationary solutions: $\left(a_0, 0, \gamma_{\rm L} k^{-2}/2\right)$ and $(0, 0, c_0)$, where a_0 and c_0 are arbitrary constants. The integrals of motions are deduced from Eqs. (5.27) as

$$a^2 + b^2 + \frac{1}{2}c^2 - \frac{\gamma_{\rm L}}{k^2}c = E_0, \tag{5.28a}$$

$$b^2 + \frac{1}{2}c^2 - \frac{\gamma_{\rm L}}{2k^2}c = E_1, \tag{5.28b}$$

$$a^2 - \frac{\gamma_{\rm L}}{2k^2}c = E_2. \tag{5.28c}$$

Similar geometrical constructions, using an ellipsoid, a cylinder and a parabola, are thus derived. (Note that one integral of motion is deduced from the other two in Eq. (5.28)). Figure 5.5 illustrates an example of the construction. Orbits are shown to be periodic. A typical orbit is illustrated by a solid curve in Fig. 5.5.

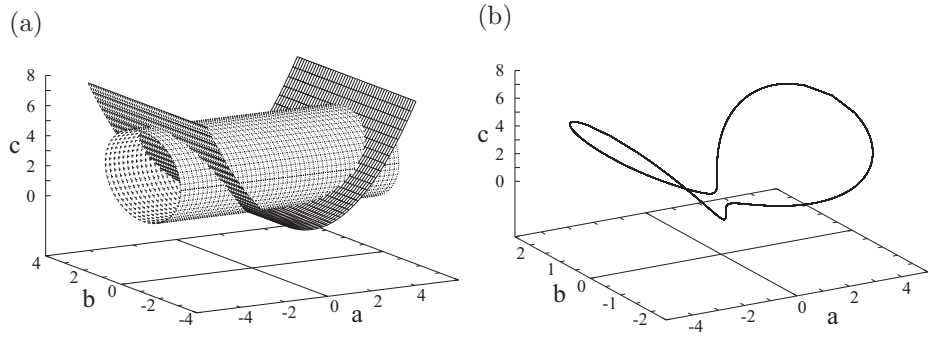

Fig. 5.5. Three-wave model for the case that includes an unstable wave. Integrals of motion are illustrated in the (a, b, c) space (a). A trajectory (the initial value of which is characterized by a small amplitude b and $a = c = 0$) is shown in (b).

5.3 The Physical Kinetics of Wave Turbulence

5.3.1 Key concepts

We now boldly leap from the *terra firma* of deterministic, integrable systems of 3 interacting modal degrees of freedom to the *terra nova* of wave turbulence—systems of N interacting waves, where $N \gg 1$. Statistical methods are required to treat such problems which involve the nonlinear interaction of many degrees of freedom. *The fundamental idea of the statistical theory of wave or weak turbulence is that energy transfer occurs by a random walk of mode couplings in the space of possible resonant interactions.* Each coupling event persists for a coherence time, which is short in comparison to the spectral evolution time. A net mode population density (i.e. energy) evolution then occurs via the accumulation of many of these short kicks or energy transfer events which add incoherently, as in a diffusion process. We remind the reader that the familiar theory of random walks and diffusion is based on:

1. two disparate time scales $\tau_{\rm ac}$, $\tau_{\rm D}$ such that $\tau_{\rm ac} \ll \tau_{\rm D}$. These are:

   a) the spectral auto-correlation time $\tau_{\rm ac}$—which corresponds to an inverse bandwidth—and sets the duration of *one* random kick or step time

   and

   b) the diffusion time $\tau_{\rm D} \sim \Delta v^2/D_v$—the time to diffuse some finite interval in velocity Δv. *Many* steps occur during one τ_D

2. an evolution equation involving a fluctuating force, i.e. $\mathrm{d}v/\mathrm{d}t = q\tilde{E}/m$ so $\delta v \sim (q/m)\,\tilde{E}\tau_{\rm ac}/m$ sets the step *size*.

Thus, $D \sim \left\langle \delta v^2 \right\rangle / \tau_{\rm ac} \sim (q/m)^2 \left\langle E^2 \right\rangle \tau_{\rm ac}$ is the diffusion coefficient which gives the rate of evolution. By analogy, we can say that the statistical theory of wave turbulence is based on

1. having two disparate time scale $\tau_{T_{\rm c}}$ and τ_E, such that $\tau_{T_{\rm c}} \ll \tau_E$. Here, the fundamental time scales correspond to
   a) the coupling or triad coherence time $\tau_{T_{\rm c}}$—which is the duration time of any specific three wave coupling. Possible triad structures are shown in Figure 5.6. $\tau_{T_{\rm c}}$ is set by the inverse bandwidth (i.e. net dispersion) of the frequency mismatch.
   b) the energy transfer time, τ_E which is analogous to γ_E^{-1} for the case of coherent coupling (γ_E: definded as Eq. (5.18).).
2. the stochastic mode population evolution equation. Here, additional assumptions such as the Random Phase Approximations are required for closure, since stochastic amplitudes mean that the noise is multiplicative, not additive, as in the case of Brownian motion.

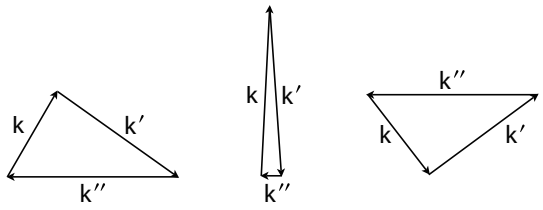

Fig. 5.6. Possible triads where $\boldsymbol{k} + \boldsymbol{k}' + \boldsymbol{k}'' = 0$

We should add here that wave turbulence or weak turbulence differs from fully developed or 'strong' turbulence, since for the latter, linear frequencies are completely washed out, so the triad coherence and energy transfer times are not distinguishable. For wave turbulence, standard perturba-

tion theory based on linear wave response is possible, while for strong turbulence, renormalization—an uncontrolled approximation which effectively sums some portion of perturbation theory to all orders—is required.

Given that $N \gg 1$, even wave turbulence theory is highly non-trivial, and several assumptions are needed to make progress. The central element of the statistical theory of wave turbulence is the *wave kinetic equation* (WKE), which is effectively a Boltzmann equation for the wave population density $N(\boldsymbol{x}, \boldsymbol{k}, t)$. Since N is proportional to the wave intensity, all phase information is lost enroute to the WKE, which is derived by utilizing a 'random phase' or 'weak coupling' approximation. Attempts at justifying the random phase approximation often invoke notions of "many modes" (i.e. $N \gg 1$) or "broad spectra", but it must be said that these criteria are rather clearly inadequate and can indeed be misleading. For example, the Kuramoto model of synchronization involves $N \gg 1$ coupled nonlinear oscillators, yet exhibits states of synchronization—perfect phase coherence in the $N \to \infty$ limit—diametrically *opposite* behavior to that of a randomly phased ensemble of waves! Simply having a large number of degrees of freedom does not—in and of itself—ensure stochasticity! A more plausible rationale for a statistical approach is to appeal to the possibility that the triad coherence time τ_{T_c} is shorter than the coherent energy transfer time τ_E, i.e. $\tau_{T_c} \ll \tau_E$. In this case, since a particular mode $\boldsymbol{k}$ will participate in many uncorrelated triad couplings prier to significant change of its population via nonlinear energy transfer, such dynamics are amenable to description as a random walk in the space of possible resonant interactions. Having $N \gg 1$ modes suggests that $M > 1$ resonant couplings or kicks can occur in the course of spectral evolution, thus permitting us to invoke the Central Limit Theorem to justify a statistical approach. Truth in advertising compels us to admit that this is

little more than a physically appealing plausibility argument though, since we have no apriori knowledge of the density of resonant triads in $\boldsymbol{k}$-space or the statistical distribution of triad coherence times. In this regard, we remark that a tail on the coherence time pdf—due to long lived triads—could be one possible indication of intermittency in wave turbulence.

5.3.2 Structure of wave kinetic equation

It is useful to heuristically survey the theory of wave turbulence prior to delivering into the technical exposition—both to see the 'big picture' and to identify key time and space scales. Since much of the structure of wave turbulence theory is analogous to that of the kinetic theory of gases (KTG), it is advantageous to discuss the theory by comparison and contrast with the KTG. Just as the Boltzmann equation (BE) evolves the one-body distribution function $f(1)$ via single particle orbits and collisions, i.e.

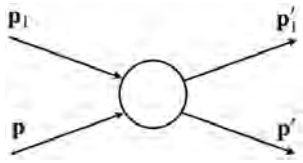

Fig. 5.7. Two-particle collision for gas kinetics.

$$\frac{\partial f}{\partial t} + Lf = C(f), \tag{5.29}$$

the wave kinetic equation (WKE) evolves the wave quanta density—usually the wave action density, given by $E_{\boldsymbol{k}}/\omega_{\boldsymbol{k}}$, according to

$$\frac{\partial N_{\boldsymbol{k}}}{\partial t} + L_{\boldsymbol{k}} N_{\boldsymbol{k}} = C\{N\}. \tag{5.30}$$

Here, L is the linear evolution operator, and $L_{\boldsymbol{k}}$ generates the evolution of N along ray trajectories. The Boltzmann collision integral (the centerpiece

of the KTG) has the structure

$$C(f) = \int \mathrm{d}\Gamma_1 \mathrm{d}\Gamma' \mathrm{d}\Gamma'_1 \, w_{\mathrm{T}} \left(f' f'_1 - f f_1 \right) \tag{5.31a}$$

where w_{T} is the transition probability for an individual scattering event (sketched in the cartoon in Fig. 5.7) and has the structure

$$w_{\mathrm{T}} \sim w \delta \left(\left(\boldsymbol{p}'_1 + \boldsymbol{p}' \right) - \left(\boldsymbol{p} + \boldsymbol{p}_1 \right) \right) \delta \left(\left(E'_1 + E' \right) - \left(E + E_1 \right) \right). \tag{5.31b}$$

Here, the delta functions enforce conservation of energy and momentum in an individual collision event and the weight w is proportioned to the collisional cross-section σ. It's useful to comment that in the relevant case of number conserving interactions with small momentum transfer (i.e. $\boldsymbol{p}' = \boldsymbol{p} - \boldsymbol{q}$, where $|\boldsymbol{q}| \ll |\boldsymbol{p}|$), $C(f)$ can be written in the form of a divergence of a flux, i.e.

$$C(f) = -\boldsymbol{\nabla}_p \cdot \boldsymbol{S}_p \tag{5.32a}$$

where the phase space flux $\boldsymbol{S}_{p_\alpha}$ is

$$\boldsymbol{S}_{p_\alpha} = \int_{q_\alpha > 0} \mathrm{d}^3 p' \mathrm{d}^3 q \, \boldsymbol{w} \left(\boldsymbol{p}, \boldsymbol{p}', \boldsymbol{q} \right) \left[\boldsymbol{f}(\boldsymbol{p}) \frac{\partial f'(\boldsymbol{p}')}{\partial \boldsymbol{p}'_\beta} - f' \left(\boldsymbol{p}' \right) \frac{\partial f(\boldsymbol{p})}{\partial \boldsymbol{p}_\beta} \right] q_\alpha q_\beta. \tag{5.32b}$$

The reader should not be surprised to discover that the collision integral in the wave kinetic equation often takes the form

$$\begin{aligned} C\{N\} = \int \mathrm{d}^3 k' \Big[\left| V_{\boldsymbol{k}', \boldsymbol{k}-\boldsymbol{k}'} \right|^2 N_{\boldsymbol{k}'} N_{\boldsymbol{k}-\boldsymbol{k}'} - \left| V_{\boldsymbol{k}, \boldsymbol{k}'} \right|^2 N_{\boldsymbol{k}'} N_{\boldsymbol{k}} \Big] \\ \times \delta \left(\boldsymbol{k}'' - \boldsymbol{k} - \boldsymbol{k}' \right) \delta \left(\omega_{\boldsymbol{k}+\boldsymbol{k}'} - \omega_{\boldsymbol{k}} - \omega_{\boldsymbol{k}'} \right), \end{aligned} \tag{5.33}$$

since the theory of wave kinetics also models pdf evolution as a sequence of many weak interactions which add incoherently. Here the transition probability w and the coupling functions $V_{\boldsymbol{k}, \boldsymbol{k}', \boldsymbol{k}''}$ parametrize the basic interaction strengths, $f(\boldsymbol{p}')$ and $N_{\boldsymbol{k}'}$ account for the distribution of 'field parti-

cles' (which scatter a given test particle) or the background mode population (which scatters a given test mode), and the factor of $\delta(\boldsymbol{k}''-\boldsymbol{k}-\boldsymbol{k}')$ $\times\delta(\omega_{\boldsymbol{k}''}-\omega_{\boldsymbol{k}}-\omega_{\boldsymbol{k}'})$ enforces momentum and energy conservation in an elementary interaction. In the case where couplings result in small increments of the test mode wave vector, $C\{N\}$ can also be simplified to the convection-diffusion form

$$C\{N\}=-\boldsymbol{\nabla}_{\boldsymbol{k}}\cdot\boldsymbol{S}_{\boldsymbol{k}}, \tag{5.34a}$$

$$S_{\boldsymbol{k}_\alpha}=V_\alpha\langle N(\boldsymbol{k})\rangle-D_{\alpha\beta}\frac{\partial\langle N\rangle}{\partial k_\beta}. \tag{5.34b}$$

Here the convection velocity V_α is usually associated with local interactions between comparable scales, and the diffusion $D_{\alpha\beta}$ (called induced diffusion) is usually due to random straining or refraction of small scales by larger ones. Both $C(f)$ and $C\{N\}$ appear as the difference of two competing terms, since both model evolution by a succession of inputs and outputs, or emissions and absorptions. Both $C(f)$ and $C\{N\}$ are derived from an *assumption* of microscopic chaos—in the case of KTG, the "Principle of Molecular Chaos" is used to justify the factorization

$$f(1,2)=f(1)f(2). \tag{5.35}$$

For wave turbulence, the Random Phase Approximation (RPA)—which approximates all modal phases as random variables (i.e. $\Phi_k=A_{\boldsymbol{k}}e^{-i\alpha_{\boldsymbol{k}}}$, with $\alpha_{\boldsymbol{k}}$ random) with Gaussian distribution allows

$$\begin{aligned}\langle\Phi_{\boldsymbol{k}_1}\Phi_{\boldsymbol{k}_2}\Phi_{\boldsymbol{k}_3}\Phi_{\boldsymbol{k}_4}\rangle&=|\Phi_{\boldsymbol{k}_1}|^2|\Phi_{\boldsymbol{k}_3}|^2\delta(\boldsymbol{k}_1-\boldsymbol{k}_2)\delta(\boldsymbol{k}_3-\boldsymbol{k}_4)+\text{symmetric term}\\&\sim N(\boldsymbol{k}_1)N(\boldsymbol{k}_3)\delta(\boldsymbol{k}_1-\boldsymbol{k}_2)\delta(\boldsymbol{k}_3-\boldsymbol{k}_4)+\text{s.t.}.\end{aligned} \tag{5.36}$$

In a related vein, $C(f)$ is derived from an assumption of diluteness or weak correlation, while $C\{N\}$ is based on a test mode hypothesis, which assumes that the statistics and other properties of all modes are similar. Table 5.1 summarizes the comparison and contrast of the KTG and wave kinetics.

One advantage of the 'preview' of wave turbulence theory given above is that we can identify the basic time scales and explore the implications of their ordering. Inspection of Eq. (5.19b) reveals the basic temporal rates;

— the mismatch frequency

$$\omega_{\mathrm{MM}} = \omega_{\boldsymbol{k}''} - \omega_{\boldsymbol{k}} - \omega_{\boldsymbol{k}'}, \tag{5.37}$$

which gives the net oscillation rate for any given triad. Obviously, $\omega_{\mathrm{MM}} \to 0$ for resonant triads. The number density of resonant triads in a given range of wave vectors is central to quantifying the efficiency of resonant interactions and determing if they are stochastic or coherent. In practice, this number density is set by the range of wave-vectors, the dissipative cut-off, and the structure of the dispersion relation.

— the rate of dispersion of ω_{MM}

$$\Delta\omega_T = \left|\frac{\mathrm{d}\omega_{\mathrm{MM}}}{\mathrm{d}k}\Delta k'\right| \cong \left|\left(\frac{\mathrm{d}\omega_{\boldsymbol{k}''}}{\mathrm{d}\boldsymbol{k}''} - \frac{\mathrm{d}\omega_{\boldsymbol{k}'}}{\mathrm{d}\boldsymbol{k}'}\right)\Delta\boldsymbol{k}'\right| \tag{5.38}$$

which gives the rate at which a particular triad disperses due to wave propagation. $\Delta\omega_T^{-1}$ is a plausible estimate for the dispersion-induced triad coherence time $\tau_{T_{\mathrm{c}}}$. It is enlightening to observe that the triad decoherence rate $\Delta\omega_T \sim |(\boldsymbol{v}_g(\boldsymbol{k}') - \boldsymbol{v}_g(\boldsymbol{k}'')) \cdot \Delta\boldsymbol{k}'|$ i.e. the typical rate at which two interacting wave packets disperse at their different group speeds. Thus, the triad coherence which enters the lifetime of mode $\boldsymbol{k}$ is set simply by the rate at which the interacting packets stream away from each other at their respective group velocities. Note also that $\Delta\omega_T \sim$

Table 5.1. *Comparison and contrast of the kinetic theory of gases and wave kinetics.*

Kinetic Theory of Gases	**Wave Kinetics**
Time Scales	
collision frequency ν_{c}	triad de-coherence rate $(1/\tau_{T_{\mathrm{c}}})$
relaxation time	spectral evolution time
Structure	
particle Liouvillian L	eikonal Liouvillian $L_{\boldsymbol{k}}$
Boltzmann $C\left(f\right)$	wave-wave interaction operator $C\left\{N_{\boldsymbol{k}}\right\}$
Landau collision operator	wave Fokker-Planck operator
cross-section σ	coupling coefficients $\left\|V_{\boldsymbol{k},\boldsymbol{k}',\boldsymbol{k}''}\right\|^2$
energy and momentum conservation factors i.e. $\delta\left(\sum \boldsymbol{P}_{\mathrm{in}} - \sum \boldsymbol{P}_{\mathrm{out}}\right)\delta\left(\sum E_{\mathrm{in}} - E_{\mathrm{out}}\right)$	selection rules for $\boldsymbol{k},\omega$ matching i.e. $\delta\left(\boldsymbol{k}'' - \boldsymbol{k} - \boldsymbol{k}'\right)\delta\left(\omega_{\boldsymbol{k}''} - \omega_{\boldsymbol{k}} - \omega_{\boldsymbol{k}'}\right)$
field particles	background, ambient waves
test particle	test wave
Irreversibility	
principle of molecular chaos	random phase approximation
micro-reversibility due detailed balance	micro-reversibility due selection rules, conservation laws
coarse graining → macro irreversibility → H-Theorem	coarse graining → macro irreversibility → H-Theorem
uniform Maxwellian equilibrium solution	Bose-Einstein, zero-flux equilibrium solution
transport → finite flux in $\boldsymbol{x}$	cascade solution → finite flux in $\boldsymbol{k}$

$\left|\left(\partial^2\omega/\partial k_\alpha \partial k_\beta\right)\Delta k_\alpha \Delta k_\beta\right|$ is related to the strength of diffraction in the waves, and is sensitive to anisotropy in dispersion.

— the energy transfer rate γ_E. For *coherent* interactions, $\gamma_E^{\rm coh}$ is similar to that given by Eq. (5.16), i.e.

$$\gamma_E^{\rm coh} \sim \left(|V|^2\,|a|^2/\omega_1\omega_2\right)^{1/2}.$$

For *stochastic* interactions in wave kinetics, we will soon see that

$$\gamma_E^{\rm stoch} \sim \sum_{\boldsymbol{k}'} V_{\boldsymbol{k},\boldsymbol{k}',\boldsymbol{k}-\boldsymbol{k}'} N_{\boldsymbol{k}'} \tau_{T_{\rm c}} \sim \left(\gamma_E^{\rm coh}\right)^2 \tau_{T_{\rm c}}. \tag{5.39}$$

Expressing the results for these two limiting cases in a consistent notation

$$\gamma^{\rm stoch}/\gamma^{\rm coh} \sim \tau_{T_{\rm c}}\gamma^{\rm coh}, \tag{5.40}$$

indicates that for comparable intensity levels, energy transfer is *slower* in wave kinetics than for coherent interaction. This is because in wave kinetics transfer occurs via a random walk of step duration $\tau_{T_{\rm c}}$, where $\tau_{T_{\rm c}} < \gamma_E^{-1}$, so many steps are required to stochastically transfer an amount of energy comparable to that transferred in a single coherent interaction. Validity of wave kinetics requires $\Delta\omega_T < \gamma_E^{\rm coh}$ *and* $\Delta\omega_T < \gamma_E^{\rm stoch}$. We again emphasize that, as in quasilinear theory, *wave dispersion* is crucial to the applicability of perturbative, weak turbulence methodology. A broad spectrum (large $|\Delta\boldsymbol{k}|$) alone is *not* sufficient for validity of wave kinetics, since in the absence of dispersion, resonant triads in that spectrum remain correlated for dynamically long times, forcing $\tau_{T_{\rm c}}\gamma^E \to 1$. This is suggestive of either nonlinear structure formation (i.e. shocks, developed by steeping), or the onset of strong turbulence.

5.3.3 'Collision' integral

Moving beyond generality, we now turn to the concrete task of constructing the collision integral for the wave kinetic equation. As with coherent interaction, this is best done via two complementary examples:

i) a general calculation for a 'generic' model evolution equation, assuming random transitions. This parallels the treatment for coherent interaction.

ii) a calculation for the specific and relevant example of the Hasegawa-Mima equation for drift-Rossby waves.

5.3.3.1 Model dynamical equation

A generic form for the nonlinear oscillator equation is

$$\frac{\mathrm{d}^2 \mathrm{a}_{\boldsymbol{k}}}{\mathrm{d}t^2} + \omega_{\boldsymbol{k}}^2 \mathrm{a}_{\boldsymbol{k}} = \sum_{\boldsymbol{k}'} V_{\boldsymbol{k},\boldsymbol{k}',\boldsymbol{k}-\boldsymbol{k}'} \mathrm{a}_{\boldsymbol{k}'} \mathrm{a}_{\boldsymbol{k}-\boldsymbol{k}'}. \tag{5.41}$$

Here, $\mathrm{a}_{\boldsymbol{k}}$ is the field variable of mode $\boldsymbol{k}$, $\omega_{\boldsymbol{k}}$ is the linear wave frequency and $V_{\boldsymbol{k},\boldsymbol{k}',\boldsymbol{k}-\boldsymbol{k}'}$ is the coupling function which ordinarily is $\boldsymbol{k}$-dependent. Here $V_{\boldsymbol{k},\boldsymbol{k}',\boldsymbol{k}-\boldsymbol{k}'}$ has the symmetries

$$V_{\boldsymbol{k},\boldsymbol{k}',\boldsymbol{k}-\boldsymbol{k}'} = V_{\boldsymbol{k},\boldsymbol{k}-\boldsymbol{k}',\boldsymbol{k}'} = V_{-\boldsymbol{k},-\boldsymbol{k}',-\boldsymbol{k}+\boldsymbol{k}'}, \tag{5.42a}$$

$$V_{\boldsymbol{k},\boldsymbol{k}',\boldsymbol{k}-\boldsymbol{k}'} = V_{\boldsymbol{k}-\boldsymbol{k}',-\boldsymbol{k}',\boldsymbol{k}} \operatorname{sgn}\left(\omega_{\boldsymbol{k}} \omega_{\boldsymbol{k}-\boldsymbol{k}'}\right). \tag{5.42b}$$

Extracting the fast oscillation, i.e.

$$\mathrm{a}_{\boldsymbol{k}}(t) = a_{\boldsymbol{k}}(t)\, e^{-i\omega_{\boldsymbol{k}} t},$$

where $a_{\boldsymbol{k}}(t)$ indicates the wave amplitude, gives

$$\frac{\mathrm{d}}{\mathrm{d}t} a_{\boldsymbol{k}}(t) = i \sum_{\boldsymbol{k}'} V_{\boldsymbol{k},\boldsymbol{k}',\boldsymbol{k}-\boldsymbol{k}'} a_{\boldsymbol{k}'}(t)\, a_{\boldsymbol{k}-\boldsymbol{k}'}(t) \exp\left[-i\left(\omega_{\boldsymbol{k}'} + \omega_{\boldsymbol{k}-\boldsymbol{k}'} - \omega_{\boldsymbol{k}}\right) t\right] \tag{5.43}$$

which may be thought of as the multi-mode counterpart of Eqs. (5.8), the modal amplitude equation. A factor of ω has been absorbed in the coupling coefficient. Here the occupation density or number of quanta for a particular mode $\boldsymbol{k}$ is $N_{\boldsymbol{k}} = |a_{\boldsymbol{k}}|^2$. Since ultimately we seek the collision operator for the evolution of $N_{\boldsymbol{k}}(t)$, we proceed by standard time-dependent perturbation theory. As the change in occupation $\Delta N_{\boldsymbol{k}}(t)$ is given by

$$\Delta N_{\boldsymbol{k}}(t) = \left\langle |a_{\boldsymbol{k}}(t)|^2 \right\rangle - \left\langle |a_{\boldsymbol{k}}(0)|^2 \right\rangle \tag{5.44a}$$

working to second order in δa, $a_{\boldsymbol{k}}(t) - a_{\boldsymbol{k}}(0) = \delta a_{\boldsymbol{k}}^{(1)} + \delta a_{\boldsymbol{k}}^{(2)} + \cdots$, gives

$$\Delta N_{\boldsymbol{k}}(t) = \left\langle \left| \delta a_{\boldsymbol{k}}^{(1)}(t) \right|^2 \right\rangle + \left\langle a_{\boldsymbol{k}}^*(0)\, \delta a_{\boldsymbol{k}}^{(2)}(t) \right\rangle + \left\langle \delta a_{\boldsymbol{k}}^{(2)*} a_{\boldsymbol{k}}(0) \right\rangle. \tag{5.44b}$$

Expanding in a straightforward manner gives:

$$\begin{aligned} \frac{\mathrm{d}}{\mathrm{d}t}\left(\delta a_{\boldsymbol{k}}^{(1)}(t) + \delta a_{\boldsymbol{k}}^{(2)}(t) + \cdots\right) &= i \sum_{\boldsymbol{k}'} V_{\boldsymbol{k},\boldsymbol{k}',\boldsymbol{k}-\boldsymbol{k}'} \left(a_{\boldsymbol{k}'}(0) + \delta a_{\boldsymbol{k}}^{(1)}\right) \\ &\quad \times \left(a_{\boldsymbol{k}-\boldsymbol{k}'}(0) + \delta a_{\boldsymbol{k}-\boldsymbol{k}'}^{(1)}\right) \exp\left[-i\left(\omega_{\boldsymbol{k}'} + \omega_{\boldsymbol{k}-\boldsymbol{k}'} - \omega_{\boldsymbol{k}}\right) t\right], \end{aligned} \tag{5.45a}$$

so

$$\delta a_{\boldsymbol{k}}^{(1)}(t) = i \sum_{\boldsymbol{k}',\boldsymbol{k}''} a_{\boldsymbol{k}'}(0)\, a_{\boldsymbol{k}''}(0) \int_0^t \mathrm{d}t'\, \hat{V}_{\boldsymbol{k},\boldsymbol{k}',\boldsymbol{k}''}\left(t'\right), \tag{5.45b}$$

where

$$\hat{V}_{\boldsymbol{k},\boldsymbol{k}',\boldsymbol{k}''}(t) = V_{\boldsymbol{k},\boldsymbol{k}',\boldsymbol{k}''} \exp\left[-i\left(\omega_{\boldsymbol{k}'} - \omega_{\boldsymbol{k}''} - \omega_{\boldsymbol{k}}\right) t\right], \tag{5.45c}$$

and we understand that $\boldsymbol{k}'' = \boldsymbol{k} - \boldsymbol{k}'$ here. Similar straightforward calculations give for $\delta a^{(2)}$:

$$\begin{aligned} \delta a_{\boldsymbol{k}}^{(2)} = -\sum_{\substack{\boldsymbol{k}',\boldsymbol{k}'' \\ \boldsymbol{q}',\boldsymbol{q}''}} \Bigg\{ & a_{\boldsymbol{k}'}(0)\, a_{\boldsymbol{q}'}(0)\, a_{\boldsymbol{q}''}(0) \int_0^t \mathrm{d}t' \int_0^{t'} \mathrm{d}t''\, \hat{V}_{\boldsymbol{k},\boldsymbol{k}',\boldsymbol{k}''}\left(t'\right) \hat{V}_{\boldsymbol{k}',\boldsymbol{q}'\boldsymbol{q}''}\left(t''\right) \\ & + a_{\boldsymbol{k}''}(0)\, a_{\boldsymbol{q}'}(0)\, a_{\boldsymbol{q}''}(0) \int_0^t \mathrm{d}t' \int_0^{t'} \mathrm{d}t'' \hat{V}_{\boldsymbol{k},\boldsymbol{k}',\boldsymbol{k}''}\left(t'\right) \hat{V}_{\boldsymbol{k}.\boldsymbol{q}',\boldsymbol{q}''}\left(t''\right) \Bigg\}. \end{aligned} \tag{5.45d}$$

In the first term on the RHS of Eq. (5.45d), $\boldsymbol{q}' + \boldsymbol{q}'' = \boldsymbol{k} - \boldsymbol{k}'$, while in the second $\boldsymbol{q}' + \boldsymbol{q}'' = \boldsymbol{k}'$.

5.3.3.2 Extraction of response and closure

To close the calculation of $\Delta N_{\boldsymbol{k}}(t)$—the change in occupation number, correlators such as $\left\langle \delta a^{(1)} \delta a^{(1)} \right\rangle$ and $\left\langle \delta a \delta a^{(2)} \right\rangle$ are simplified by the Random Phase Approximation (RPA). The essence of the RPA is that if the duration of phase correlations is *shorter than any other time scale in the problem*, then the phases of the modal amplitude may be taken as random, i.e.

$$a_{\boldsymbol{k}} \to \hat{a}_{\boldsymbol{k}} e^{i\theta_{\boldsymbol{k}}}$$

with $\theta_{\boldsymbol{k}}$ random. Then, for

$$\langle \quad \rangle = \langle \quad \rangle_{\text{ensemble}} = \int \mathrm{d}\theta \, P(\theta) \,,$$

where $P(\theta)$ is the pdf of phase $\theta_{\boldsymbol{k}}$,

$$\begin{aligned} \langle a_{\boldsymbol{k}} a_{\boldsymbol{k}'} \rangle &= \left\langle \hat{a}_{\boldsymbol{k}} e^{i\theta_{\boldsymbol{k}}} \hat{a}_{\boldsymbol{k}'} e^{i\theta_{\boldsymbol{k}'}} \right\rangle \\ &= |\hat{a}_{\boldsymbol{k}}|^2 \, \delta_{\boldsymbol{k},-\boldsymbol{k}'} \end{aligned} \tag{5.46a}$$

and

$$N_{\boldsymbol{k}} = |\hat{a}_{\boldsymbol{k}}|^2 \,. \tag{5.46b}$$

We should comment that:

i) the RPA should be considered as arising from the need to close the moment hierarchy. Truly random phases of the physical modal amplitudes would preclude any energy transfer, since all triad couplings would necessarily vanish. Rather, the RPA states that modal correlations are in some sense weak, and induced only via nonlinear interaction of resonant triads,

ii) the RPA is an uncontrolled approximation. It lacks rigorous justification and cannot predict its own error.

iii) the RPA is seemingly relevant to a system with short triad coherence time (i.e. $\gamma_E \tau_{T_c} \ll 1$), and so it should be most applicable to ensembles of waves where many strongly dispersive waves resonantly interact, though this connection has not been firmly established.

Having stated all those caveats, we must add that there is no way to make even the crudest, most minimal progress on wave turbulence without utilizing the RPA. It is the *only* game in town.

Closure modelling is explained in detail in the next chapter, and we discuss here the extraction of interaction time briefly. Proceeding, the increment in occupation ΔN driven by weak coupling can thus be written as

$$\begin{aligned}\Delta N_{\boldsymbol{k}}(t) = \\ \Bigg\langle \mathrm{Re} \sum_{\substack{\boldsymbol{k}',\boldsymbol{k}'' \\ \boldsymbol{q}',\boldsymbol{q}''}} \Bigg\{ & a_{\boldsymbol{k}'}(0)\, a_{\boldsymbol{k}''}(0)\, a^*_{\boldsymbol{q}'}(0)\, a^*_{\boldsymbol{q}''}(0) \int_0^t \mathrm{d}t'\, \hat{V}_{\boldsymbol{k},\boldsymbol{k}',\boldsymbol{k}''}(t') \int_0^t \mathrm{d}t''\, \hat{V}^*_{\boldsymbol{k},\boldsymbol{q}',\boldsymbol{q}''}(t'') \\ & - a_{\boldsymbol{k}}(0)\, a_{\boldsymbol{k}'}(0)\, a^*_{\boldsymbol{q}'}(0)\, a^*_{\boldsymbol{q}''}(0) \int_0^t \mathrm{d}t'\, \hat{V}_{\boldsymbol{k},\boldsymbol{k}',\boldsymbol{k}''}(t') \int_0^t \mathrm{d}t''\, \hat{V}^*_{\boldsymbol{k}'',\boldsymbol{q}',\boldsymbol{q}''}(t'') \\ & - a_{\boldsymbol{k}}(0)\, a_{\boldsymbol{k}''}(0)\, a^*_{\boldsymbol{q}'}(0)\, a^*_{\boldsymbol{q}''}(0) \int_0^t \mathrm{d}t'\, \hat{V}_{\boldsymbol{k},\boldsymbol{k}',\boldsymbol{k}''}(t') \int_0^t \mathrm{d}t''\, \hat{V}^*_{\boldsymbol{k}',\boldsymbol{q}',\boldsymbol{q}''}(t'') \Bigg\} \Bigg\rangle .\end{aligned} \tag{5.47}$$

Since the bracket refers to an average over phase, we can factorize and reduce the averages of quartic products by the requirement of phase matching. For example, the first term on the RHS of Eq. (5.47) may be written as:

$$\Delta N_1 = \sum_{\substack{\boldsymbol{k}',\boldsymbol{k}'' \\ \boldsymbol{q}',\boldsymbol{q}''}} \left\langle a_{\boldsymbol{k}'}(0)\, a_{\boldsymbol{k}''}(0)\, a^*_{\boldsymbol{q}'} a^*_{\boldsymbol{q}''} \right\rangle \int_0^t \mathrm{d}t'\, \hat{V}_{\boldsymbol{k},\boldsymbol{k}',\boldsymbol{k}''}(t') \int_0^t \mathrm{d}t''\, \hat{V}^*_{\boldsymbol{k},\boldsymbol{q}',\boldsymbol{q}''}(t'') , \tag{5.48a}$$

where possible factorizations of the quartic product are given by:

$$\left\langle a_{\mathbf{k}'}(0)\, a_{\mathbf{k}''}(0)\, a^*_{\mathbf{q}'} a^*_{\mathbf{q}''}\right\rangle \rightarrow \left\langle a_{\mathbf{k}'}(0)\, a_{\mathbf{k}''}(0)\, a^*_{\mathbf{q}'} a^*_{\mathbf{q}''}\right\rangle$$

$$= \left|\hat{a}_{\boldsymbol{k}'}\right|^2 \delta_{\boldsymbol{k}',\boldsymbol{q}'} \left|\hat{a}_{\boldsymbol{k}''}\right|^2 \delta_{\boldsymbol{k}'',\boldsymbol{q}''} + \left|\hat{a}_{\boldsymbol{k}'}\right|^2 \delta_{\boldsymbol{k}',\boldsymbol{q}''} \left|\hat{a}_{\boldsymbol{k}''}\right|^2 \delta_{\boldsymbol{k}'',\boldsymbol{q}'}.$$

Thus

$$\begin{aligned}\Delta N_1 = &\sum_{\boldsymbol{k}',\boldsymbol{k}''} N_{\boldsymbol{k}'} N_{\boldsymbol{k}''} \int_0^t \mathrm{d}t'\, \hat{V}_{\boldsymbol{k},\boldsymbol{k}',\boldsymbol{k}''}\left(t'\right) \int_0^t \mathrm{d}t''\, \hat{V}^*_{\boldsymbol{k},\boldsymbol{k}',\boldsymbol{k}''}\left(t''\right) \\ &+ \sum_{\boldsymbol{k}',\boldsymbol{k}''} N_{\boldsymbol{k}'} N_{\boldsymbol{k}''} \int_0^t \mathrm{d}t'\, \hat{V}_{\boldsymbol{k},\boldsymbol{k}',\boldsymbol{k}''}\left(t'\right) \int_0^t \mathrm{d}t''\, \hat{V}^*_{\boldsymbol{k},\boldsymbol{k}'',\boldsymbol{k}'}\left(t''\right).\end{aligned} \tag{5.48b}$$

Using the coupling function symmetries as given by Eq. (5.42), simple but tedious manipulation then gives

$$\Delta N_1 = 2 \sum_{\boldsymbol{k}',\boldsymbol{k}''} N_{\boldsymbol{k}'} N_{\boldsymbol{k}''} \left[\int_0^t \mathrm{d}t'\, \hat{V}^*_{\boldsymbol{k},\boldsymbol{k}',\boldsymbol{k}''}\left(t'\right) \int_0^t \mathrm{d}t''\, \hat{V}_{\boldsymbol{k},\boldsymbol{k}',\boldsymbol{k}''}\left(t''\right)\right]. \tag{5.49}$$

To perform the time integration, as in the case of Brownian motion it is convenient to transform to relative ($\tau = (t' - t'')/2$) and average ($T = (t' + t'')/2$) time variables and then symmetrize to obtain

$$\begin{aligned}&\left[\int_0^t \mathrm{d}t' \hat{V}^*_{\boldsymbol{k},\boldsymbol{k}',\boldsymbol{k}''}\left(t'\right) \int_0^t \mathrm{d}t'' \hat{V}_{\boldsymbol{k},\boldsymbol{k}',\boldsymbol{k}''}\left(t''\right)\right] \\ &= \left|V_{\boldsymbol{k},\boldsymbol{k}',\boldsymbol{k}''}\right|^2 2 \int_0^t \mathrm{d}T \int_0^T \mathrm{d}\tau \exp\left[i\left(\omega_{\boldsymbol{k}} - \omega_{\boldsymbol{k}'} - \omega_{\boldsymbol{k}''}\right)\tau\right] \qquad (5.50a) \\ &= \left|V_{\boldsymbol{k},\boldsymbol{k}',\boldsymbol{k}''}\right|^2 2 \int_0^t \mathrm{d}T \frac{\left(\exp\left(i\left(\omega_{\boldsymbol{k}} - \omega_{\boldsymbol{k}'} - \omega_{\boldsymbol{k}''}\right)T\right) - 1\right)}{i\left(\omega_{\boldsymbol{k}} - \omega_{\boldsymbol{k}'} - \omega_{\boldsymbol{k}''}\right)}\end{aligned}$$

so taking $T \gg \omega_{\mathrm{MM}}^{-1}, \Delta\omega_{\mathrm{MM}}^{-1}$ then gives

$$= 2\pi t \left|V_{\boldsymbol{k},\boldsymbol{k}',\boldsymbol{k}''}\right|^2 \delta\left(\omega_{\boldsymbol{k}} - \omega_{\boldsymbol{k}'} - \omega_{\boldsymbol{k}''}\right). \tag{5.50b}$$

Equation (5.50) has the classic structure of a transition probability element, as given by the Fermi Golden Rule for incoherent couplings induced by

time-dependent perturbations. Here the time dependency arises from the limited duration of the triad coherence set by the dispersion in ω_{MM}. ΔN is in proportion to t. Since t is, by construction, large in comparison to any other time scale in the problem, as in Fokker-Planck theory we can write,

$$\frac{\partial N_1}{\partial t} = 4\pi \sum_{\boldsymbol{k}',\boldsymbol{k}''} N_{\boldsymbol{k}'} N_{\boldsymbol{k}''} \left|V_{\boldsymbol{k},\boldsymbol{k}',\boldsymbol{k}''}\right|^2 \delta\left(\omega_{\boldsymbol{k}} - \omega_{\boldsymbol{k}'} - \omega_{\boldsymbol{k}''}\right). \tag{5.51}$$

A similar set of calculations for the second and third terms on the RHS then gives the total collision integral for population evolution due to stochastic wave-wave interaction with short coherence time as

$$\begin{aligned} C\left\{N_{\boldsymbol{k}}\right\} =& 4\pi \sum_{\boldsymbol{k}',\boldsymbol{k}''} \left(V_{\boldsymbol{k},\boldsymbol{k}',\boldsymbol{k}''}\right)^2 \delta_{\boldsymbol{k},\boldsymbol{k}',\boldsymbol{k}''} \delta\left(\omega_{\boldsymbol{k}} - \omega_{\boldsymbol{k}'} - \omega_{\boldsymbol{k}''}\right) \\ & \times \left[N_{\boldsymbol{k}'} N_{\boldsymbol{k}''} - \left(\mathrm{sgn}\left(\omega_{\boldsymbol{k}}\omega_{\boldsymbol{k}''}\right) N_{\boldsymbol{k}'} + \mathrm{sgn}\left(\omega_{\boldsymbol{k}}\omega_{\boldsymbol{k}'}\right) N_{\boldsymbol{k}''}\right) N_{\boldsymbol{k}}\right]. \end{aligned} \tag{5.52a}$$

A related form of $C\left\{N_{\boldsymbol{k}}\right\}$ with more general symmetry properties is

$$\begin{aligned} C\left\{N_{\boldsymbol{k}}\right\} =& \pi \sum_{\boldsymbol{k}',\boldsymbol{k}''} \Big\{ \left|V_{\boldsymbol{k},\boldsymbol{k}',\boldsymbol{k}''}\right|^2 \left(N_{\boldsymbol{k}'} N_{\boldsymbol{k}''} - \left(N_{\boldsymbol{k}'} + N_{\boldsymbol{k}''}\right) N_{\boldsymbol{k}}\right) \\ & \times \delta\left(\boldsymbol{k} - \boldsymbol{k}' - \boldsymbol{k}''\right) \delta\left(\omega_{\boldsymbol{k}} - \omega_{\boldsymbol{k}'} - \omega_{\boldsymbol{k}''}\right) \\ & + 2\left|V_{\boldsymbol{k}',\boldsymbol{k},\boldsymbol{k}''}\right|^2 \left(N_{\boldsymbol{k}''} N_{\boldsymbol{k}} - N_{\boldsymbol{k}'}\left(N_{\boldsymbol{k}''} + N_{\boldsymbol{k}}\right)\right) \\ & \times \delta\left(\boldsymbol{k}' - \boldsymbol{k} - \boldsymbol{k}''\right) \delta\left(\omega_{\boldsymbol{k}'} - \omega_{\boldsymbol{k}} - \omega_{\boldsymbol{k}''}\right) \Big\}. \end{aligned} \tag{5.52b}$$

The factor of 2 arises from the arbitrary choice of $\boldsymbol{k}'$ to interchange with $\boldsymbol{k}$ in the second term. The full wave kinetic equation is then

$$\frac{\partial N}{\partial t} + \left(\boldsymbol{v}_{\mathrm{gr}} + \boldsymbol{v}\right) \cdot \boldsymbol{\nabla} N - \frac{\partial}{\partial \boldsymbol{x}}\left(\omega + \boldsymbol{k} \cdot \boldsymbol{v}\right) \cdot \frac{\partial N}{\partial \boldsymbol{k}} = 2\gamma_{\boldsymbol{k}} N_{\boldsymbol{k}} + C\left\{N_{\boldsymbol{k}}\right\}. \tag{5.53}$$

Here $\boldsymbol{v}$ is an ambient large scale shear flow which advects the interacting wave population and $\gamma_{\boldsymbol{k}}$ is the linear growth or damping rate for the wave population. The LHS of Eq. (5.53) is conservative—i.e. can be written in the form $\mathrm{d}N/\mathrm{d}t$—and describes evolving N along Hamiltoninan ray trajec-

tories (see Fig.5.8)

$$\frac{\mathrm{d}\boldsymbol{x}}{\mathrm{d}t} = \boldsymbol{v}_{\mathrm{gr}} + \boldsymbol{v}, \qquad \frac{\mathrm{d}\boldsymbol{k}}{\mathrm{d}t} = -\frac{\partial\left(\omega + \boldsymbol{k}\cdot\boldsymbol{v}\right)}{\partial \boldsymbol{x}}.$$

Equation (5.52) gives the collision integral for stochastic wave-wave interaction by random triad couplings of short duration, and constitutes a central result in the theory of wave-wave interactions.

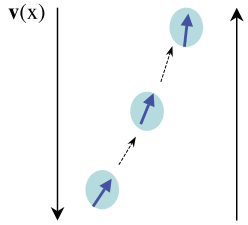

Fig. 5.8. Wave packet (which is denoted by the shade) with wave vector $\boldsymbol{k}$ (thick solid arrow) moves in the presence of large-scale strain field $\boldsymbol{v}\,(x)$. Thin dotted arrows show motion of a packet in real space.

Equation (5.52), (5.53) certainly merit discussion in detail.

→ $C\{N\}$ has the characteristic structure indicating evolution of the population $N_{\boldsymbol{k}}$ at a given wave vector $\boldsymbol{k}$ via a competition between input by (incoherent) noise and relaxation by nonlinear couplings which produce outflow to other $\boldsymbol{k}'$s, i.e.

$$\frac{\partial N}{\partial t} \sim \sum |V|^2 \Big\{ \underbrace{N_{\boldsymbol{k}'} N_{\boldsymbol{k}''}}_{\begin{array}{l}\text{— noise/incoherent}\\ \text{emission INTO } \boldsymbol{k}\\ \text{from } \boldsymbol{k}', \boldsymbol{k}''\\ \text{interaction}\\ \text{— not} \sim N_{\boldsymbol{k}}\end{array}} - (\quad) \underbrace{N_{\boldsymbol{k}'} N_{\boldsymbol{k}}}_{\begin{array}{l}\text{— relaxation OUTFLOW}\\ \text{from } \boldsymbol{k} \text{ via}\\ \text{nonlinear interaction}\\ \text{— } \sim N_{\boldsymbol{k}}\end{array}} \Big\}.$$

This structure is common to virtually *all* wave kinetic equations.

→ The population outflow or damping term in Eq. (5.53) identifies the characteristic nonlinear relaxation rate of a test mode $\boldsymbol{k}$ in wave turbulence

theory, as $\partial N_{\boldsymbol{k}}/\partial t \sim -N_{\boldsymbol{k}}/\tau_{\mathrm{R}\boldsymbol{k}}$, where the relaxation rate $1/\tau_{\mathrm{R}\boldsymbol{k}}$ is

$$1/\tau_{\mathrm{R}\boldsymbol{k}} \sim \sum_{\boldsymbol{k}',\boldsymbol{k}'} \left|V_{\boldsymbol{k},\boldsymbol{k}',\boldsymbol{k}''}\right|^2 \delta_{\boldsymbol{k},\boldsymbol{k}',\boldsymbol{k}''} \delta\left(\omega_{\boldsymbol{k}''} - \omega_{\boldsymbol{k}'} - \omega_{\boldsymbol{k}}\right) N_{\boldsymbol{k}'}$$
$$\sim \sum_{\substack{\boldsymbol{k}' \\ \text{resonant}}} \left|V_{\boldsymbol{k},\boldsymbol{k}'}\right|^2 \tau_{T_{\mathrm{c}}\boldsymbol{k}} N_{\boldsymbol{k}'}.$$

Notice that the relaxation rate is set by:

— the resonance condition and the number of resonant triads involving the test mode $\boldsymbol{k}$

— the coherence time $\tau_{T_{\mathrm{c}}\boldsymbol{k}}$ of triads involving the test mode $\boldsymbol{k}$

— the mean square coupling strength and the ambient mode intensity.

The relaxation rate $1/\tau_{\mathrm{R}\boldsymbol{k}}$ is the stochastic counterpart of the coherent energy decay rate γ_E^{coh}. Most estimates of solution levels and transport in weak turbulence theory are derived by the balance of some linear growth rate $\gamma_{\mathrm{L},\boldsymbol{k}}$ with $1/\tau_{\mathrm{R}\boldsymbol{k}}$. This gives a generic scaling of the form for a fluctuation level

$$N \sim \left(\gamma_{\mathrm{L}}/\tau_{T_{\mathrm{c}}}\right) \left|V_{\boldsymbol{k},\boldsymbol{k}'}\right|^{-2}$$

→ $C\{N\}$ conserves the spectrum integrated wave energy $\mathcal{E}$ ($\mathcal{E} = N\omega$) and momentum $\boldsymbol{P}$ ($\boldsymbol{P} = N\boldsymbol{k}$) densities since the resonance conditions enforce these conservation laws in the microscopic interactions. In the case where the scattering increment ($\Delta\boldsymbol{k}$) of the test mode is small, so $C\{N\} \rightarrow -\boldsymbol{\nabla}_{\boldsymbol{k}} \cdot \boldsymbol{S}_{\boldsymbol{k}}$, $C\{N\}$ also conserves excitation *number*. In general, however, the Manley-Rowe relations tell us that total exciton number need not be conserved in three mode interactions—i.e. two waves in, one out (or the reverse)—though it is for the case of resonant four-wave processes (i.e. two in → two out).

→ As should be apparent from the triad resonance conditions, $C\{N\}$ sup-

ports several types of wave-wave interaction processes, depending on dispersion, coupling strength and behavior, etc. Interactions can be local in $\boldsymbol{k}$, in which case $C\{N\}$ takes the generic form

$$C\{N\} = -\frac{\partial}{\partial \boldsymbol{k}}\left(\boldsymbol{V}\left(\boldsymbol{k}, N\right) N_{\boldsymbol{k}}\right)$$

as in the Leith model of turbulence. Here $\boldsymbol{V}\left(\boldsymbol{k}, N\right)$ represents a flux or flow of quanta density in wave vector. Interactions can be non-local in $\boldsymbol{k}$ but proceed via small $\Delta\boldsymbol{k}$ increments, in which case $\boldsymbol{S_k}$ is diffusive, i.e.

$$\boldsymbol{S_k} = -\mathsf{D}_{\boldsymbol{k}}\frac{\partial N}{\partial \boldsymbol{k}}$$

so

$$C\{N\} = \frac{\partial}{\partial \boldsymbol{k}}\mathsf{D}_{\boldsymbol{k}}\frac{\partial N_{\boldsymbol{k}}}{\partial \boldsymbol{k}}.$$

Such interaction are referred to as *induced diffusion*. The physics of certain generic classes of non-local wave interactions including induced diffusion, will be discussed later in this chapter.

→ Given the parallel development of wave kinetics and the kinetic theory of gas, its no surprise that one can construct and prove an H-theorem for $C\{N\}$ in analogy to the Boltzmann H-theorem. Here, the entropy is

$$\mathcal{S} = \int \mathrm{d}\boldsymbol{k}\, \ln\left(N_{\boldsymbol{k}}\right) \tag{5.54}$$

and the distribution for which $\mathrm{d}\mathcal{S}/\mathrm{d}t = 0$ corresponds to a Rayleigh-Jeans type distribution, $N_{\boldsymbol{k}} = T/\omega_{\boldsymbol{k}}$. This implies that equipartition of energy is one stationary population distribution $N_{\boldsymbol{k}}$ in the limit $\omega_{\boldsymbol{k}} \ll T$. This equilibrium distribution corresponds to a state of zero spectral flux or energy dissipation rate. The theory of entropy production in wave turbulence is developed further in the monograph by Zakharov, et.al. (Zakharov et al., 1992), and discussed furthur in the next chapter.

5.3.4 Application to drift-Rossby wave

Proceeding as in our discussion of coherent wave-wave interactions, we now present the theory of wave kinetics for the very relevant case of drift-Rossby wave turbulence in its simplest incarnation, namely the Hasegawa-Mima equation. There are several reasons for explicit consideration of this example, which include:

— the relevance of drift-Rossby wave turbulence to confinement physics
— the impact of the dual conservation of energy and potential enstrophy—both quadratic invariant of moments—on the wave spectrum evolution
— the consequent appearance of 'negative viscosity phenomena'—i.e. the tendency of wave energy to be scattered toward large scale.
— the relation of wave interaction to potential vorticity transport.
— the breaking of scale in variance in the coupling factors, on account of $k_\perp \rho_\mathrm{s}$ independence.

5.3.4.1 Model

The quasi-geostrophic or Hasegawa-Mima equation for drift-Rossby waves is

$$\frac{\mathrm{d}}{\mathrm{d}t}\left(F\phi - \nabla^2\phi\right) + V_\mathrm{de}\frac{\partial\phi}{\partial y} = 0 \tag{5.55a}$$

where advection is by $\boldsymbol{E}\times\boldsymbol{B}$ velocity

$$\frac{\mathrm{d}}{\mathrm{d}t} = \frac{\partial}{\partial t} + \boldsymbol{\nabla}\phi\times\hat{z}\cdot\boldsymbol{\nabla}. \tag{5.55b}$$

So for mode $\boldsymbol{k}$, we have the generic amplitude evolution equation

$$\frac{\partial\phi_{\boldsymbol{k}}(t)}{\partial t} + i\omega_{\boldsymbol{k}}\phi_{\boldsymbol{k}}(t) = \sum_{\boldsymbol{k}'+\boldsymbol{k}''=\boldsymbol{k}} V_{\boldsymbol{k},\boldsymbol{k}',\boldsymbol{k}''}\phi_{\boldsymbol{k}'}(t)\,\phi_{\boldsymbol{k}''}(t) \tag{5.56a}$$

where the coupling coefficient is

$$V_{\boldsymbol{k},\boldsymbol{k}',\boldsymbol{k}''} = \frac{1}{2}\frac{\left(\boldsymbol{k}'\cdot\boldsymbol{k}''\times\hat{z}\right)\left(k''^2-k'^2\right)}{F+k^2} \tag{5.56b}$$

and the drift wave frequency is just

$$\omega_{\boldsymbol{k}} = k_y V_{\mathrm{de}}/\left(F+k_\perp^2\right). \tag{5.57}$$

Derivation and explanation for the model equation (5.55) are given in the Appendix. Equation (5.56a) is the basic equation for the evolution of modal amplitudes $\phi_{\boldsymbol{k}}(t)$. The long time evolution of the wave intensity $|\phi_{\boldsymbol{k}}|^2$ due to nonlinear couplings is given by the triad correlator i.e.

$$\frac{\partial}{\partial t}\left|\phi_{\boldsymbol{k}}(t)\right|^2 = \sum_{\boldsymbol{k}'+\boldsymbol{k}''=\boldsymbol{k}} V_{\boldsymbol{k},\boldsymbol{k}',\boldsymbol{k}''}\left\langle\phi_{\boldsymbol{k}}^*(t)\,\phi_{\boldsymbol{k}'}(t)\,\phi_{\boldsymbol{k}''}(t)\right\rangle = T_{\boldsymbol{k}}. \tag{5.58}$$

The triad correlater $T_{\boldsymbol{k}}$ is non-vanishing due to test wave couplings which survive the ensemble average over random phases denoted by the brackets $\langle\ \ \rangle$, and which satisfy the resonance condition. Hence,

$$T_{\boldsymbol{k}} = \sum_{\boldsymbol{k}'+\boldsymbol{k}''=\boldsymbol{k}} V_{\boldsymbol{k},\boldsymbol{k}',\boldsymbol{k}''}\Bigg[\underbrace{\left\langle\phi_{\boldsymbol{k}'}(t)\,\phi_{\boldsymbol{k}''}(t)\,\delta\phi_{\boldsymbol{k}}^{*(2)}(t)\right\rangle}_{\text{incoherent emission } T_1} + \underbrace{\left\langle\phi_{\boldsymbol{k}}(t)\,\delta\phi_{\boldsymbol{k}''}^{(2)}\phi_{\boldsymbol{k}}^*(t)\right\rangle}_{\text{relaxation } T_2} + \underbrace{\left\langle\delta\phi_{\boldsymbol{k}'}^{(2)}(t)\,\phi_{\boldsymbol{k}''}(t)\,\phi_{\boldsymbol{k}}^*(t)\right\rangle}_{\text{relaxation } T_2}\Bigg] \tag{5.59}$$

where in the first term, which ultimately represents nonlinear noise or incoherent emission,

$$\delta\phi_{\boldsymbol{k}}^{(2)} \sim \phi_{\boldsymbol{k}'}\phi_{\boldsymbol{k}''}, \quad \text{so} \quad T_{1\boldsymbol{k}} \sim \left|\phi_{\boldsymbol{k}'}\right|^2\left|\phi_{\boldsymbol{k}-\boldsymbol{k}'}\right|^2$$

and the second two ultimately represent nonlinear relaxation i.e.

$$\delta\phi_{\boldsymbol{k}''}^{(2)} \sim \phi_{\boldsymbol{k}'}\phi_{\boldsymbol{k}}, \quad \text{so} \quad T_{2\boldsymbol{k}} \sim \left|\phi_{\boldsymbol{k}'}\right|^2\left|\phi_{\boldsymbol{k}}\right|^2.$$

To complement our derivation of Eq. (5.52), here we will explicitly calculate T_2—the nonlinear relaxation response—and simply state the result for the incoherent contribution to $T_{\boldsymbol{k}}$. For the nonlinear response contribution T_2, after symmetrization, etc. we straightforwardly obtain

$$T_{2\boldsymbol{k}} = \sum_{\boldsymbol{k}'} \left(\frac{\boldsymbol{k}' \cdot \boldsymbol{k} \times \hat{z}}{F + k^2} \right) \left(k''^2 - k'^2 \right) \left\langle \phi_{-\boldsymbol{k}}(t) \, \phi_{-\boldsymbol{k}'}(t) \, \delta\phi^{(2)}_{\boldsymbol{k}+\boldsymbol{k}'}(t) \right\rangle \tag{5.60a}$$

and

$$\frac{\partial}{\partial t} \delta\phi^{(2)}_{\boldsymbol{k}+\boldsymbol{k}'} + i\omega_{\boldsymbol{k}+\boldsymbol{k}'} \delta\phi^{(2)}_{\boldsymbol{k}+\boldsymbol{k}'} = \left(\frac{\boldsymbol{k}' \cdot \boldsymbol{k} \times \hat{z}}{F + k''^2} \right) \left(k'^2 - k^2 \right) \phi_{\boldsymbol{k}'}(t) \, \phi_{\boldsymbol{k}}(t) \tag{5.60b}$$

so

$$\delta\phi^{(2)}_{\boldsymbol{k}+\boldsymbol{k}'} = \int_{-\infty}^{t} \mathrm{d}t' \, \exp\left[i\omega_{\boldsymbol{k}+\boldsymbol{k}'} \left(t - t' \right) \right] \left(\frac{\boldsymbol{k}' \cdot \boldsymbol{k} \times \hat{z}}{F + k''^2} \right) \left(k'^2 - k^2 \right) \phi_{\boldsymbol{k}'}\left(t' \right) \phi_{\boldsymbol{k}}\left(t' \right). \tag{5.60c}$$

Causality and $t > t'$ together imply that $\omega_{\boldsymbol{k}+\boldsymbol{k}} \to \omega + i\epsilon$, so ϕ^2 is damped at $t \to -\infty$. Combining all this gives the T_2 contribution

$$\begin{aligned} T_{2\boldsymbol{k}} = \sum_{\boldsymbol{k}'} & \frac{\left(\boldsymbol{k}' \cdot \boldsymbol{k} \times \hat{z} \right)^2}{\left(F + k^2 \right) \left(F + k''^2 \right)} \left(k''^2 - k'^2 \right) \left(k'^2 - k^2 \right) \\ & \times \int_{-\infty}^{t} \mathrm{d}t' \, \exp\left[i\omega_{\boldsymbol{k}+\boldsymbol{k}'} \right] \left\langle \phi_{-\boldsymbol{k}}(t) \, \phi_{-\boldsymbol{k}'}(t) \, \phi_{\boldsymbol{k}'}(t) \, \phi_{\boldsymbol{k}}\left(t' \right) \right\rangle. \end{aligned} \tag{5.61}$$

We further take the two time correlator as set by wave frequency, nonlinear dynamics and causality, alone. This allows the two time scale ansatz

$$\left\langle \phi^*_{\boldsymbol{k}}(t) \, \phi_{\boldsymbol{k}'}\left(t' \right) \right\rangle = \left| \phi_{\boldsymbol{k}}\left(t' \right) \right|^2 \delta_{\boldsymbol{k}+\boldsymbol{k}',0} \exp\left[-i\omega_{\boldsymbol{k}} \left(t - t' \right) \right] \tag{5.62}$$

since $t' > t$, $\omega \to \omega + i\epsilon$ guarantees that correlation decays as $t \to \infty$. It is understood that the amplitude varies slowly relative to the phase. Using

Eq. (5.62) in Eq. (5.61) then gives

$$T_{2\boldsymbol{k}} = \sum_{\boldsymbol{k}'} \frac{\left(\boldsymbol{k}\cdot\boldsymbol{k}'\times\hat{z}\right)^2}{\left(F+k^2\right)\left(F+k'^2\right)} \left(k''^2-k'^2\right)\left(k'^2-k^2\right)\left|\phi_{\boldsymbol{k}'}\right|^2\left|\phi_{\boldsymbol{k}}\right|^2\Theta_{\boldsymbol{k},\boldsymbol{k}',\boldsymbol{k}''},$$

(5.63a)

where Θ, the triad coherence time, is

$$\Theta_{\boldsymbol{k},\boldsymbol{k}',\boldsymbol{k}''} = \int_{-\infty}^{t} \mathrm{d}t' \, \exp\left[-i\left(\omega_{\boldsymbol{k}}+\omega_{\boldsymbol{k}'}-\omega_{\boldsymbol{k}''}\right)\left(t-t'\right)\right] \tag{5.63b}$$

and $\boldsymbol{k}''=\boldsymbol{k}+\boldsymbol{k}'$ taking the real part finally gives (for weak nonlinear interaction)

$$\mathrm{Re}\,\Theta_{\boldsymbol{k},\boldsymbol{k}',\boldsymbol{k}''} = \pi\delta\left(\omega_{\boldsymbol{k}}+\omega_{\boldsymbol{k}'}-\omega_{\boldsymbol{k}''}\right), \tag{5.63c}$$

from where appears the resonant coupling condition. Hence, the nonlinear response contribution to T is

$$T_{2\boldsymbol{k}} = \sum_{\boldsymbol{k}'} \frac{\left(\boldsymbol{k}\cdot\boldsymbol{k}'\times\hat{z}\right)^2}{\left(F+k^2\right)\left(F+k''^2\right)} \left(k''^2-k'^2\right)\left(k'^2-k^2\right) \times\left|\phi_{\boldsymbol{k}'}\right|^2\left|\phi_{\boldsymbol{k}}\right|^2\pi\delta\left(\omega_{\boldsymbol{k}}+\omega_{\boldsymbol{k}'}-\omega_{\boldsymbol{k}''}\right). \tag{5.64}$$

T_1—the noise emission part of the spectral transfer— can similarly shown to be

$$T_{1\boldsymbol{k}} = \sum_{\substack{\boldsymbol{p},\boldsymbol{q}\\ \boldsymbol{p}+\boldsymbol{q}=\boldsymbol{k}}} \frac{\left(\boldsymbol{p}\cdot\boldsymbol{q}\times\hat{z}\right)^2}{\left(F+k^2\right)^2}\left(q^2-p^2\right)\left(q^2-p^2\right) \times\left|\phi_{\boldsymbol{p}}\right|^2\left|\phi_{\boldsymbol{q}}\right|^2\pi\delta\left(\omega_{\boldsymbol{k}}-\omega_{\boldsymbol{p}}-\omega_{\boldsymbol{q}}\right) \tag{5.65}$$

so

$$T_{\boldsymbol{k}} = T_{1\boldsymbol{k}} + T_{2\boldsymbol{k}}. \tag{5.66}$$

Several aspects of Eqs. (5.64) and (5.65) merit detailed discussion.

→ The relaxation time $\tau_{\mathrm{R},\boldsymbol{k}}$ can be read off directly from Eq. (5.64) as

$$1/\tau_{\mathrm{R},\boldsymbol{k}} = \sum_{\boldsymbol{k}'} \frac{\left(\boldsymbol{k}\cdot\boldsymbol{k}'\times\hat{z}\right)^2}{\left(1+k^2\right)\left(1+k''^2\right)} \left(k''^2-k'^2\right)\left(k^2-k'^2\right) \times \left|\phi_{\boldsymbol{k}'}\right|^2 \pi\delta\left(\omega_{\boldsymbol{k}}+\omega_{\boldsymbol{k}'}-\omega_{\boldsymbol{k}''}\right). \quad (5.67)$$

For $|\boldsymbol{k}| \ll |\boldsymbol{k}'|$, $1/\tau_{\mathrm{R},\boldsymbol{k}} < 0$, while for $|\boldsymbol{k}| \gg |\boldsymbol{k}'|$ as usual, $1/\tau_{\mathrm{R},\boldsymbol{k}} > 0$. This is suggestive of 'inverse transfer' or a 'negative viscosity' phenomenon, whereby intensity is scattered to large scales from smaller scales. This is a recurring theme in 2D and drift-Rossby turbulence and follows from the dual conservation of energy and potential enstrophy. 2D and geostrophic turbulence dynamics is discussed in Chapter 2, while geostrophic turbulence is discussed further in Chapter 6 and in Volume II. The reader should be cautioned here that "negative viscosity" refers only to the tendency of the system to scatter energy to large *scale*. A patch of turbulence in such systems tends to broaden and spread itself in space by scattering via mutual induction of the interacting vortices. (See Fig. 5.9 for illustration.) Also, while the dynamics of negative viscosity phenomena in drift-Rossby wave turbulence resembles that of the inverse cascade, familiar from 2D fluids, we stress that these two are *not* identical. Wave turbulence dynamics depends sensitively on triad resonance and thus on dispersion, etc. and transfer of energy need not be local in $\boldsymbol{k}$. The inverse cascade is a local process in $\boldsymbol{k}$, and is insensitive to the details of wave dynamics. Further discussion is given in Chapter 7.

→ The conservation property for the transfer function $T_{\boldsymbol{k}}$ must be noted.

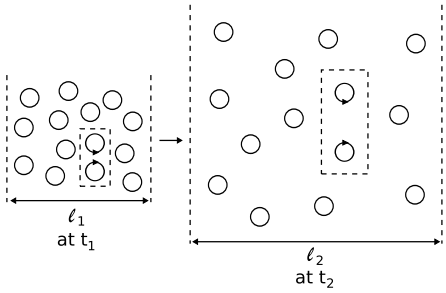

Fig. 5.9. Broadening or spreading ($l_2 > l_1$, $t_2 > t_1$) of a patch of 2D turbulence by mutual induction of vortex motion.

One can straightforwardly show that

$$\sum_{\boldsymbol{k}} \left(F + k^2\right) T_{\boldsymbol{k}} = 0$$

$$\sum_{\boldsymbol{k}} \left(F + k^2\right)^2 T_{\boldsymbol{k}} = 0$$

so both energy E and potential enstrophy Ω

$$E = \sum_{\boldsymbol{k}} \left(1 + k^2\right) |\phi_{\boldsymbol{k}}|^2$$

$$\Omega = \sum_{\boldsymbol{k}} \left(1 + k^2\right)^2 |\phi_{\boldsymbol{k}}|^2$$

are conserved by the wave coupling process. (See also the explanation of conservation in the Appendix.) Note that proper treatment of both noise and nonlinear response is required for balance of the energy and potential enstrophy budgets. In particular, potential enstrophy conservation is manifested in wave kinetics from the direct correlation between nonlinear noise and response terms. Conservation is a simple consequence of symmetrization of the perturbation theory and is not an especially discriminating test of a turbulence theory.

→ In general, drift wave dispersion is quite strong, so resonant triads are,

in the same sense, rather 'special'. This is due at least in part, to the gyro/Rossby radius dependence (i.e. $k_\perp^2\rho_i^2$ factor (ρ_i: ion gyro radius)) in the dispersion relation, which breaks scale invariance. An exception to this occurs at long wavelength, i.e. $k^2 \ll F$ (i.e. $k_\perp^2\rho_i^2 < 1$), where $\omega_{\boldsymbol{k}} \sim (k_y V_{\rm de}/F)\left(1 - k_\perp^2/F\right)$ (i.e. $\omega_{\boldsymbol{k}} \sim k_y V_{\rm de}\left(1 - k_\perp^2\rho_i^2\right)$), so the waves are nearly dispersion free. There $\tau_{T_c} \sim O\left(F/k^2\right)$ (i.e. $\sim O\left(1/k^2\rho_i^2\right)$), so the triad coherence diverges and renormalization is definitely required. The general structure of resonant triads for Rossby wave turbulence was considered by Longuet-Higgins and Gill (Longuet-Higgins et al., 1967), and we refer the reader to that original source for further discussion. We do remark, though, that if one of the interacting modes is a low frequency or zero frequency shear flow (i.e. a Zonal flow or GAM (Diamond et al., 2005b)), resonance occurs much more easily. This is one reason for the dominant role of zonal flows in drift wave turbulence. This topic will be extensively descussed in Volume II.

5.3.5 Issues to be considered

After this introduction to the derivation and structure of the theory of wave kinetics, it is appropriate to pause to take stock of the situation and to reflect on what *has* and *has not* been accomplished. So far, we have developed a perturbative, statistical theory of wave population evolution dynamics. Indeed, by construction the structure of wave kinetics closely resembles the theory for incoherent emission and absorption of photons in atomic transitions and the theory of vibrational mode interactions in a solid. Wave kinetics is built upon the dual assumptions of negligible mode-mode coherency (i.e. the RPA) and short triad lifetime ($\tau_{T_c}\gamma_E < 1$), and so is limited in

applicability to system of a large number of dispersive waves. Wave kinetics *does*

— provide a framework within which we may identify and assess nonlinear interaction mechanisms and with which to calculate mode population evolution

— preserve relevant energy, momentum etc. conservation properties of the primitive equations. We emphasize that this is not an especially rigorous test of the theory, however.

— provide a collision operator $C\{N\}$ for the wave kinetic equation which enables the construction of radiation hydrodynamic equations for the wave momentum and energy fields, etc.

— enable the identification of relevant time and space scales. However, from the trivial solution of energy equipartition, we have *not* yet:

→ demonstrated the actual existence of any solutions to the wave kinetic equation which annihilate $C\{N\}$

→ characterized the class of possible local and non-local interactions and their impact on spectral evolution

→ considered the stability of possible solutions.

We now turn to these issues.

5.4 The Scaling Theory of Local Wave Cascades

5.4.1 Basic ideas

We now turn from the formal development of wave interaction theory to discuss:

— how one might actually *use* wave kinetics to calculate the wave spectrum.

We discuss several examples of wave cascades

— solutions of the WKE with finite spectral flux

— the relation of local cascades in wave turbulence to the K41 theory discussed in Chapter 2.

Truth in advertising compels us to admit the wave kinetic equation is rarely solved outright, except in a few very simple and rather academic cases. Given its complexity, this should be no surprise. Instead, usually its structure is analyzed to determine which types of coupling mechanisms are dominant, and how to construct a *simpler* dynamical model of spectral evolution for that particular case. In this section, we present some instructive 'studies' in this approach. For these, wave kinetics plays an important role as a general structure within which to determine relaxation time. Sadly though, there is no universal solution. Rather, the form of the dispersion relation and compling coefficients make each case a challenge and opportunity.

5.4.1.1 Fokker-Planck approach

We begin by examining processes which produce a small increment in the wave vector $\boldsymbol{k}$. Here, *small increment* refers to couplings between roughly comparable scales or $\boldsymbol{k}$ values, which results in a slight shift $\Delta\boldsymbol{k}$ in the test mode wave-vector. The Kolmogorov (K41) cascade is a classic example of a *small increment process* in scale space. For small increments, one might think of N (N: action density in k space) evolving as in a Fokker-Planck process, i.e.

$$N\left(t+\Delta t,\boldsymbol{k}\right)=\int \mathrm{d}\Delta\boldsymbol{k}\, N\left(t,\boldsymbol{k}-\Delta\boldsymbol{k}\right) T\left(\Delta\boldsymbol{k},\Delta t\right), \tag{5.68a}$$

where $T(\Delta\boldsymbol{k}, \Delta t)$ is the transition probability for a step or k-increment of size $\Delta\boldsymbol{k}$ in a time interval Δt. The usual algebra then gives

$$\begin{aligned}\frac{\partial N_{\boldsymbol{k}}}{\partial t} &= -\frac{\partial}{\partial \boldsymbol{k}} \cdot \left\{ \left\langle \frac{\mathrm{d}\boldsymbol{k}}{\mathrm{d}t} \right\rangle N - \frac{\partial}{\partial \boldsymbol{k}} \cdot \left\langle \frac{\Delta\boldsymbol{k}\Delta\boldsymbol{k}}{2\Delta t} \right\rangle N \right\} \\ &= -\frac{\partial}{\partial \boldsymbol{k}} \cdot \left\{ (\boldsymbol{V}_{\boldsymbol{k}} N) - \frac{\partial}{\partial \boldsymbol{k}} \cdot (\mathsf{D}_{\boldsymbol{k}} N) \right\},\end{aligned} \tag{5.68b}$$

where

→ $\boldsymbol{V}_{\boldsymbol{k}} = \langle \mathrm{d}\boldsymbol{k}/\mathrm{d}t \rangle$ is the mean 'flow velocity' in $\boldsymbol{k}$. This flux in $\boldsymbol{k}$ results from a series of small increments $\Delta\boldsymbol{k}$, as shown in Fig. 5.10.

→ $\mathsf{D}_{\boldsymbol{k}} = \langle \Delta\boldsymbol{k}\Delta\boldsymbol{k}/2\Delta t \rangle$ is the $\boldsymbol{k}$-space diffusivity which describes evolution of the $\boldsymbol{k}$-variance of N.

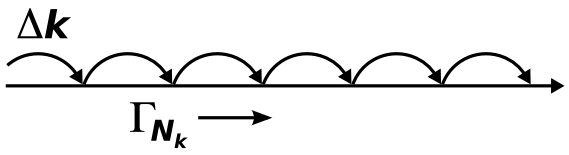

Fig. 5.10. Flux of $N_{\boldsymbol{k}}$ induced by a series of small increments in steps $\Delta\boldsymbol{k}$.

Since the flow and diffusion in $\boldsymbol{k}$ are produced by mode-mode interactions, obviously $\boldsymbol{V}_{\boldsymbol{k}} = \boldsymbol{V}_{\boldsymbol{k}}\{N\}$, $\mathsf{D}_{\boldsymbol{k}} = \mathsf{D}_{\boldsymbol{k}}\{N\}$. Sources (i.e. growth) and sinks (i.e. damping) may also be added to Eq.(5.41). While $\boldsymbol{k}$-space diffusion is a small increment process, it is in general *not* a local one. Rather, the strain field driving $\mathsf{D}_{\boldsymbol{k}}$ usually is localized at larger and slower scales than those of the test wave. For local interactions producing a net mean exciton flux in $\boldsymbol{k}$-space, the lowest order description of a small increment process simply neglects diffusion and, in the absence of sources and sinks, reduces to

$$\frac{\partial N_{\boldsymbol{k}}}{\partial t} + \frac{\partial}{\partial \boldsymbol{k}} \cdot (\boldsymbol{V}_{\boldsymbol{k}} N_{\boldsymbol{k}}) = 0. \tag{5.69a}$$

Here, the stationary spectrum is just that which produces a divergence-free flux in $\boldsymbol{k}$—i.e. that for which

$$\frac{\partial}{\partial \boldsymbol{k}} \cdot (\boldsymbol{V}_{\boldsymbol{k}} N_{\boldsymbol{k}}) = 0. \tag{5.69b}$$

5.4.1.2 Leith model

Frequently, it is useful to formulate the flux in a 1D (i.e. scalar) $\boldsymbol{k}$-space, or scale (i.e. l) space. In such cases, the relaxation rate $\sim 1/\tau_{\mathrm{R}k}$ is often easier to construct than a flow velocity. When the spectrum is isotropic, N_k depends only on $k = |\boldsymbol{k}|$, the one dimensional density$N(k) = 4\pi k^2 N_{\boldsymbol{k}}$ is used, and a measure of the wave number quanta within the wave number k,

$$\mathcal{n}(k) = kN(k),$$

is introduced. The velocity in the k-space is also specified by a scalar variable $V(k)$, which denotes the velocity in the $|\boldsymbol{k}|$-direction. In the next step, the velocity in the k-space $V(k)$ is rewritten in terms of the relaxation rate as,

$$\frac{1}{k} V(k) = \frac{\mathrm{d}}{\mathrm{d}t} \ln k \sim \frac{1}{\tau_{\mathrm{R}k}}. \tag{5.70a}$$

Rewriting the divergence operator $(\partial/\partial \boldsymbol{k}) \cdot$ in one-dimensional form $k^{-2} (\mathrm{d}/\mathrm{d}k) k^2$, Eq.(5.69a) is rewritten as

$$\frac{\partial}{\partial t} \mathcal{n}(k) + \frac{\mathrm{d}}{\mathrm{d} \ln k} \left(\frac{1}{\tau_{\mathrm{R}k}} \mathcal{n}(k) \right) = 0. \tag{5.70b}$$

The stationary spectrum satisfies

$$\frac{\mathrm{d}}{\mathrm{d}k} \left(\frac{1}{\tau_{\mathrm{R}k}} \mathcal{n}(k) \right) = 0. \tag{5.71}$$

This is the idea underpinning the Leith model, a useful and generalizable approach to modelling cascades and local processes. The Leith model, which is motivated by analogy with radiation and neutron transport theory, aims to represent the cascade's flux of energy in $\boldsymbol{k}$-space as a simple, local nonlinear

diffusion process. Such a representation is extremely useful for applications to multi-scale modelling, transport, wave radiation hydrodynamics, etc. Of course, other assumptions or physics information is required to determine V_k or $1/\tau_{\mathrm{R}k}$ and relate them to $N_{\boldsymbol{k}}$. Wave kinetic theory provides a framework with which to determine these quantities.

Like most things in turbulence theory, the Leith model is motivated by the K41 theory of Navier-Stokes turbulence, which balances local energy flux through scale l at the rate $v(l)/l$ with a constant dissipation rate ϵ, taken to be independent of scale and viscosity. Thus, we recall that

$$\epsilon = \frac{E(l)}{\tau(l)} = \frac{v^3(l)}{l}$$

or equivalently in k-space

$$\epsilon = \left[kE(k)\right]\left[k^3E(k)\right]^{1/2}.$$

Here $E(k)$ is in the 1D spectrum, so $kE(k)$ is a measure of the energy in wavenumber k and $\left[k^3E(k)\right]^{1/2} = k\left[kE(k)\right]^{1/2} = 1/\tau_{\mathrm{R}k}$ is just the eddy turn-over rate. In essence, k appears as a density-of-states factor. Hence, $E(k) \sim \epsilon^{2/3}k^{-5/3}$, so we recover the familiar K41 spectrum, which has finite, constant spectral energy flux ϵ. Now in the Leith model of fluid turbulence, the effective quanta density $\mathcal{n}(k)$ is just $kE(k)$, the relaxation rate is $1/\tau_{\mathrm{R}k} = \left[k^3E(k)\right]^{1/2}$ and so Eq. (5.71) is just

$$\frac{\partial}{\partial \ln k}\left(k\left(kE(k)\right)^{3/2}\right) = \frac{\partial}{\partial \ln k}\left(k^{5/2}E(k)^{3/2}\right) = 0, \tag{5.72}$$

the solution of which recovers the K41 spectrum.

5.4.1.3 Leith model with dissipation

It is instructive to discuss a slightly more complicated example of the Leith model, in order to get a feel for spectral flow constructions in a familiar

context. Retaining viscous damping as an explicit high-k sink changes the Leith model spectral flow continuity equation to

$$\frac{\partial}{\partial t}\mathcal{n}(k) + \frac{\partial}{\partial \ln k}\left(k\mathcal{n}(k)^{3/2}\right) + \nu k^2 \mathcal{n}(k) = 0. \tag{5.73}$$

Here $\mathcal{n}(k) = kE(k)$. The stationary state spectrum must then balance spectral flux and dissipation to satisfy

$$\frac{\partial}{\partial \ln k}\left(k\mathcal{n}(k)^{3/2}\right) + \nu k^2 \mathcal{n}(k) = 0,$$

with an initial condition (influx condition) that at k_0, the stirring or input wavenumber, $\mathcal{n}(k_0) = v_0^2$. Then taking $U = k\mathcal{n}(k)^{3/2}$ (note U is just the energy flow rate!) transforms the flow equation to

$$\frac{\mathrm{d}U(k)}{\mathrm{d}k} + \nu k^{1/3} U(k)^{2/3} = 0, \tag{5.74}$$

so

$$U(k) = \epsilon - \nu k^{4/3}/4. \tag{5.75}$$

In the inertial range, $\epsilon \gg \nu k^{4/3}/4$, so $U(k) = \epsilon$, $\mathcal{n}(k) = (\epsilon/k)^{2/3}$ and $E(k) = \epsilon^{2/3}k^{-5/3}$, the familiar Kolmogorov spectrum. Observe that in the Leith model, the energy dissipation rate ϵ appears as a constant of integration. Matching the boundary condition at k_0 requires $U(k_0) = k_0\mathcal{n}(k_0)^{3/2} = k_0 v_0^3 \sim v_0^3/l_0$. This gives the integration constant ϵ as

$$\begin{aligned} \epsilon &= U(k_0) + \nu k_0^{4/3}/4 \\ &\cong k_0 v_0^3. \end{aligned} \tag{5.76}$$

The second term on the RHS is just a negligible $O(1/R_e)$ correction to the familiar formula which relates the dissipation rate to the stirring scale parameters. (R_e: Reynolds number. Illustration is given in Fig. 5.11.)

From this simple example, we see that the essence of the Leith model ap-

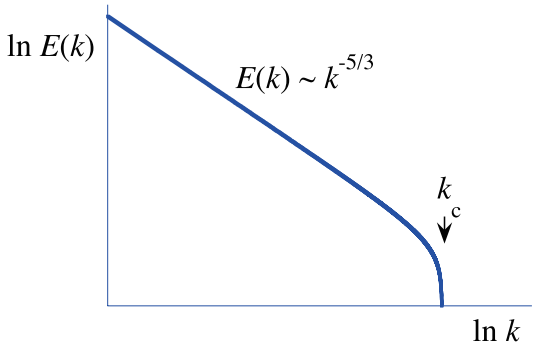

Fig. 5.11. Leith model with small but finite molecular viscosity ν. Spectrum is cut at k_c, which satisfies the relation $k_c = (4\epsilon/\nu)^{3/4}$.

proach, which is useful and applicable *only* for local, steady small increment processes, is to

→ identify an exciton density which 'flows' in k or scale space by local increments. The relevent quantity is usually suggested by some indication of self-similarity (i.e. a power-law spectrum over a range of scales).

→ use physics input or insight to identify a flow rate or relaxation time and, in particular, its depedence on $N_{\boldsymbol{k}}$. Wave kinetics is very helpful here.

→ impose stationarity to determine the spectrum. A quanta source and sink must be identified, and the necessary constant of integration is usually related to the net flow rate.

5.4.2 Gravity waves

Another instructive application of wave kinetics is to the spectrum of surface gravity waves (Lighthill, 1978). Indeed, three of the earliest and best known studies of wave kinetics are the pioneering works of Phillips (Phillips, 1966), Hasselman (Hasselmann, 1962; Hasselmann, 1968), and Zakharov and Filonenko (Zakharov and Filonenko, 1967), all of which dealt with surface wave

turbulence. Ocean surface gravity waves are excited by the wind, and continuously fill a range of scales with wavenumber $k_{\mathrm{w}} < k < k_{\mathrm{cap}}$. Here k_{w} is the wave number of the wind wave $k_{\mathrm{w}} = g/v_{\mathrm{w}}^2$, and k_{cap} is set by the small scale where surface tension becomes important, i.e. $k_{\mathrm{cap}} \sim (\rho g/\sigma)^{1/2}$ (where σ is the coefficient of surface tension, g is the gravitational acceleration, and ρ is the mass density). The surface wave displacement spectrum is a power law over this range, and asymptotes to a quasi-universal form $\left|\tilde{\xi}\right|^2 \sim k^{-4}$, at the upper end of the gravity wave range (ξ: displacement of surface). This universal spectrum is referred to as the 'Phillips spectrum,' after O.

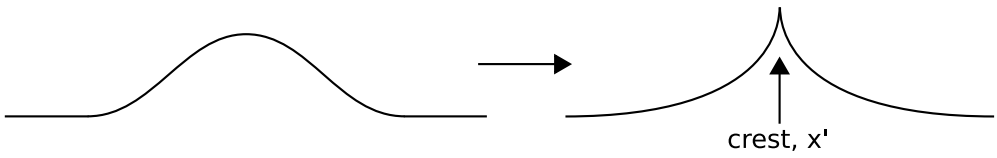

Fig. 5.12. Formation of wave slope discontinuity at crest of breaking wave. $\mathrm{d}\tilde{s}/\mathrm{d}x = \delta\,(x - x')$

M. Phillips, who first proposed it in 1955. The basic idea of the Phillips model is that the waves are saturated, i.e. sitting just at the threshold of breaking, so the wave slope $\tilde{s}$ is discontinuous, i.e. $\mathrm{d}\tilde{s}/\mathrm{d}x = \delta\,(x - x')$ at a wave crest (see Fig. 5.12). Since $\tilde{s} = k\tilde{\xi}$, this implies a displacement spectrum of $\left|\tilde{\xi}\right|^2 \sim 1/k^4$, the essence of the Phillips model. Intensive studies by a variety of sensing and analysis techniques all indicate that

— the excitations on the ocean surface are very well approximated by an ensemble of surface waves, with a power law spectrum of wave slopes.

— the Phillips spectrum is a good fit, at least at the upper end of the gravity wave range.

The scale invariance of gravity waves on the interval $k_{\rm w} < k < k_{\rm cap}$, the universality of the Phillips spectrum, and the strong excitation of gravity waves by even modest wind speeds have all combined to motivate application of the theory of wave kinetics to the problem of the gravity wave spectrum, in the hope of developing a first principles of theory. Gravity waves have several interesting features which distinguish them from Alfvén or drift waves, and which also make this example especially instructive. In particular:

— on account of the gravity wave dispersion relation $\omega = \sqrt{gk}$, there are no three-wave resonant couplings among gravity waves. Rather, the fundamental resonant interaction is *four-wave coupling*. Resonant three-wave coupling *is* possible among two gravity waves and a very small gravity-capillary wave. Indeed, the absence of the three-wave resonance among gravity waves is one likely reason why they are seemingly such a good model for ocean surface excitations.

— unlike Alfvén waves in incompressible MHD, gravity waves can break, so applicability of weak turbulence theory requires that wave displacement $\tilde{\xi}$ be small enough so that the wave slope is subcritical to breaking (i.e. $k\tilde{\xi} < 1$). This imposes a limit on the wave amplitudes and energies which are compatible with wave kinetics. More generally, it is plausible to expect the weak turbulence spectrum to be 'softer' than the Phillips spectrum (i.e. $\sim k^{-\alpha}$, $\alpha < 4$), since resonant four-wave coupling is not as efficient as wave breaking in disposing of wave energy. (Fig. 5.13)

Given the self-similar power law structure of the gravity wave spectrum, it is natural to try to model gravity wave interaction as a local energy cascade from large (wind-wave scale) to small (gravity-capillary wave scale) scales. In this sense, the gravity wave energy cascade resembles the Kolmogorov

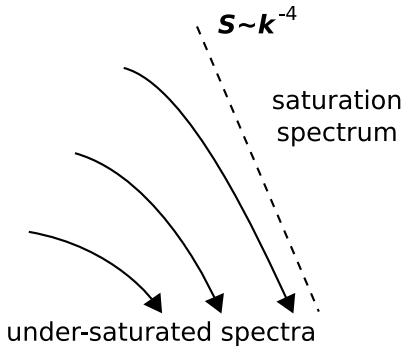

Fig. 5.13. Spectral steepening as waves approach saturation at the Phillips spectrum $S \sim k^{-4}$.

cascade. An important difference between these two cascades is the nature of the effective dissipation which terminates them. Instead of viscosity as for ordinary Navier-Stokes turbulence, the gravity wave cascade terminates by some combination of wave crest instability and wave breaking, which involves the combined effects of surface tension, vorticity at the surface layer, and the dynamics of air-sea interaction (i.e. white capping, foam and bubble formation, etc.). The dissipative dynamics of the gravity wave cascade remains an open question. Indeed, it is interesting to note that in both Kolmogorov turbulence and gravity wave turbulence, a fractal distribution of singular structures forms on the smallest scales. These may be thought of as vortex tubes and sheets for K41, and to marginally breaking wave crests or a foam of small bubbles for ocean waves. Also, in neither case does a rigorous understanding of the dissipation rate exist at present. That said, motivated by the empirical self-similarity of ocean wave turbulence, we will plunge ahead boldly and impose constant energy flux as

$$\epsilon = \frac{kE(k)}{\tau_{\mathrm{R}k}}.$$

Here, it is understood that the system is 2D, so $kE(k)$ is energy/area. The relaxation time is determined by four considerations, namely:

— that the dynamics are scale invariant and self-similar

— that the characteristic transfer rate is proportional to the surface wave frequency $\omega_{\boldsymbol{k}} = \sqrt{gk}$—the only temporal rate in the gravity wave range.

— that the fundamental interaction is four-wave coupling, so $1/\tau_{\mathrm{R}k} = [kE(k)]^2$ —i.e. an extra power of energy appears, as compared to three-wave coupling.

— that the waves must be subcritical to breaking, i.e. fluid parcel velocities v_k should be less than the wave phase ω/k ($v_k < \omega/k$), so $kE(k) < \rho_{\mathrm{w}}(\omega^2/k^2)k$. Nonlinear transfer must thus be small in the ratio $E(k)(\omega/k)^{-2}\rho_{\mathrm{w}}^{-1}$. Here ρ_{w} is the density of water and the additional factor of k^{-1} appears since $kE(k)$ has dimensions of energy/area. The particular association of length with wavelength follows from the fact that ocean wave perturbations decay exponentially with depth as $\sim e^{-|kz|}$.

Assembling these pieces enables us to construct the spectral flow equation (with ϵ constant)

$$\epsilon = \frac{kE(k)}{\tau_{\mathrm{R}k}}, \tag{5.77a}$$

where

$$\frac{1}{\tau_{\mathrm{R}k}} = \left(\frac{kE(k)}{\rho_{\mathrm{w}}\left(\omega^2/k^2\right)k}\right)^2 \omega_k, \tag{5.77b}$$

i.e. the relaxation rate is the wave frequency, multiplied by *two* powers (four-wave interaction!) of intensity, normalized to the breaking threshold. Thus, the spectral transfer equation is

$$\epsilon = \omega_{\boldsymbol{k}} \left(\frac{kE(k)}{\rho_{\mathrm{w}}\left(\omega^2/k^2\right)k}\right)^2 \left(kE(k)\right). \tag{5.78}$$

Subsequently using the dispersion relation $\omega = \sqrt{gk}$ gives $E(k) \sim k^{-5/2}$ and a surface displacement spectrum $\left|\tilde{\xi}(k)\right|^2 \sim k^{-7/2}$. This does *not* agree with the scaling of the Phillips spectrum, nor should it, since the latter is based on a hypothesis of saturation by wave breaking, which is outside the 'event horizon' of weak turbulence theory! It is indeed reassuring to see that the weak turbulence gravity wave spectrum is softer than the Phillips spectrum (i.e. $\alpha = 7/2 < 4$), as we expect. The self-similar gravity wave spectrum $\left|\tilde{\xi}(k)\right|^2 \sim k^{-7/2}$, sometimes referred to as the 'Kolmogorov spectrum' for gravity waves by Zakharov and collaborators (Zakharov et al., 1992), might be relevant to regimes where waves are driven weakly, slightly above the wind excitation threshold. Certainly, it cannot properly describe the process of wave spectrum saturation at high wind speed. Indeed, no attempt to connect the Phillips spectrum to perturbation theory or wave turbulence theory has yet succeeded, though recent efforts by Newell and Zakharov (Newell and Zakharov, 2008) appear promissing in this respect. We include this example here as an illustration of how to apply wave turbulence theory to obtain results for a more complex problem. The applications of wave kinetics to Alfvén and gravity wave turbulence are summarized in Table 5.2. (See Chapter 9 for detailed explanation of Alfvén wave turbulence.)

5.5 Non-Local Interaction in Wave Turbulence

No doubt the reader who has persevered this far is thinking, "Surely not *all* wave interaction processes are simply local cascades!?" Such skepticism is now to be rewarded as we turn to the important and often-neglected subject of non-local interaction in wave turbulence. Non-local interaction in wave turbulence refers to the resonant interaction processes of three waves

Table 5.2. *Elements of local wave cascade models*

Constituent	
Alfvén wave	gravity wave
$\omega = k_{\parallel} v_{\mathrm{A}}$	$\omega = \sqrt{kg}$
incompressible MHD	surface of ocean
Interaction	
3-wave	4-wave
Basic Rate	
$\dfrac{v^2(x_\perp)}{l_\perp^2\left(\Delta k_{\parallel} v_{\mathrm{A}}\right)}$	$\omega_k \left(\dfrac{kE(k)}{\rho_{\mathrm{w}}\left(\omega^2/k^2\right)k}\right)^2$
Constraint Limit	
critical balance	sub-critical to breaking
$\Delta k_{\parallel} v_{\mathrm{A}} \sim v(l_\perp)/l_\perp$	$kE(k) < \rho_{\mathrm{w}}\left(\omega^2/k^2\right)k$
Spectral Balance	
$\epsilon = \dfrac{v^2(l_\perp)\, v(l_\perp)}{l_\perp^2\left(\Delta k_{\parallel} v_{\mathrm{A}}\right)}$	$\alpha \equiv \omega(k)\left(\dfrac{kE(k)}{\rho_{\mathrm{w}}\left(\omega^2/k^2\right)k}\right)^2 kE(k)$
Limiting Result	
$k_{\parallel} \sim \dfrac{\epsilon^{1/3} k_\perp^{2/3}}{v_{\mathrm{A}}}$	$\lvert\tilde{\varepsilon}(k)\rvert^2 \sim k^{-7/2}$
$E(k)$ ala K41	softer than Phillips

in which the magnitudes of the three frequencies and/or wave vectors are not comparable. These are contrasted with local interactions in the cartoon of Fig. 5.6 (left). Crudely put, in local interactions, the triangles defined by resonant triad $\boldsymbol{k}$ vectors are nearly equilateral, while those corresponding to non-local interaction deviate markedly from equilateral structure, as shown in Fig. 5.6 (center). Local interactions transfer exciton density (i.e. energy) between neighboring $\boldsymbol{k}$, while non-local interaction can transfer energy between quite disparate scales—as occurs when large scale shears strain smaller

scales, for example. However, non-local interaction *is* compatible with the notion of a "small-increment process," as discussed earlier. Indeed, we shall see that stochastic shearing by large scales produces a random walk in $\boldsymbol{k}$ space at small scales—a classic example of non-local interaction resulting in a small increment, diffusive scattering of the population density.

5.5.1 Elements in disparate scale interaction

We have already encoutered one generic example of a non-local wave interaction process, namely the decay or parametric subharmonic instability in a resonant triad, discussed in section 5.2 of this chapter. There, a populated high frequency mode at $\omega \sim 2\Omega$ decays to two daughter waves at $\omega \sim \Omega$. Note that this mechanism requires a *population inversion*—the occupation density of the pump, or high frequency mode, must exceed those of the daughters in order for decay to occur. Another generic type of interaction is *induced diffusion*—an interaction where large scale, low-frequency waves strain smaller, higher-frequency waves. Induced diffusion arises naturally when one leg of the resonant triad is much shorter than the other two, indicative of a near self-beat interaction of two short-wavelength, high-frequency waves with one long-wavelength, low-frequency wave. Thus, the interaction triad is a thin, nearly isoceles triangle, as shown in Fig. 5.6 (center). The "diffusion" in induced diffusion occurs in $\boldsymbol{k}$-space, and is a consequence of the spatio-temporal scale disparity between the interacting waves. This allows an eikonal theory description of the interaction between the long-wavelength strain field and the short-wavelength mode with wave vector $\boldsymbol{k}$, which undergoes refractive scattering. Thus since

$$\frac{\mathrm{d}\boldsymbol{k}}{\mathrm{d}t} = -\boldsymbol{\nabla}\left(\omega + \boldsymbol{k}\cdot\boldsymbol{v}\right), \tag{5.79a}$$

$\delta\boldsymbol{k}$, the excursion in $\boldsymbol{k}$ due to inhomogeneities in $\omega_{\boldsymbol{k}}$ and v, is

$$\frac{\mathrm{d}}{\mathrm{d}t}\delta\boldsymbol{k} = -\boldsymbol{\nabla}\left(\tilde{\omega} + \boldsymbol{k}\cdot\tilde{\boldsymbol{v}}\right), \tag{5.79b}$$

(see Fig. 5.14 for illustration. (Diamond et al., 2005b)) So

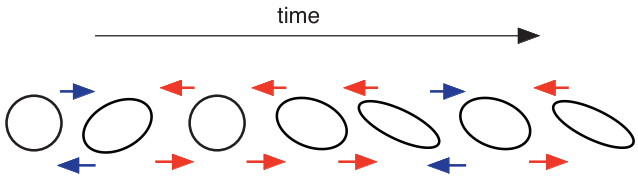

Fig. 5.14. Distortion of a small-scale perturbation (shown by circular or elliptic vortex) by an ambient large-scale sheared flow. The large scale flow changes its sign so that the wave vector of small scale perturbation is subject to diffusive change.

$$\mathsf{D}_k = \frac{\mathrm{d}}{\mathrm{d}t}\left\langle\delta\boldsymbol{k}^2\right\rangle = \sum_q \boldsymbol{q}\boldsymbol{q}\left|\left(\tilde{\omega} + k\cdot\tilde{v}\right)_q\right|^2 \tau_{\boldsymbol{k},\boldsymbol{q}}, \tag{5.80}$$

where $\tau_{\boldsymbol{k},\boldsymbol{q}}$ is the coherence time of the scattering field $\boldsymbol{q}$ with the scattered ray $\boldsymbol{k}$. Insight into the physics of $\tau_{\boldsymbol{k},\boldsymbol{q}}$ follows from consideration of the triad resonance function in the limit where $|\boldsymbol{q}| \ll \boldsymbol{k}, \boldsymbol{k}'$, i.e.

$$\begin{aligned}\Theta_{\boldsymbol{k},\boldsymbol{k}',\boldsymbol{q}} &= \frac{i}{\omega_{\boldsymbol{q}} + \omega_{\boldsymbol{k}'} - \omega_{\boldsymbol{k}'+\boldsymbol{q}}} \\ &\simeq \frac{i}{\omega_{\boldsymbol{q}} + \omega_{\boldsymbol{k}'} - \omega_{\boldsymbol{k}'} - \boldsymbol{q}\cdot\left(\partial\omega_{\boldsymbol{k}'}/\partial\boldsymbol{k}'\right)} \\ &= \frac{i}{\omega_{\boldsymbol{q}} - \boldsymbol{q}\cdot v_{\mathrm{gr}}(\boldsymbol{k})},\end{aligned} \tag{5.81a}$$

so

$$\mathrm{Re}\,\Theta_{\boldsymbol{k},\boldsymbol{k}',\boldsymbol{q}} \cong \pi\delta\left(\omega_{\boldsymbol{q}} - \boldsymbol{q}\cdot v_{\mathrm{gr}}(\boldsymbol{k})\right). \tag{5.81b}$$

Hence, the coherence time $\tau_{\boldsymbol{k},\boldsymbol{q}}$ is set by larger of:

— the dispersion rate of the strain field spectrum (i.e. the q's), as "seen" by

a wavepacket with group velocity $v_{\rm gr}(k)$, i.e.

$$\frac{1}{\tau_{{\rm ac},\boldsymbol{q},\boldsymbol{k}}} = \left| \left(\frac{{\rm d}\omega_{\boldsymbol{q}}}{{\rm d}\boldsymbol{q}} - \boldsymbol{v}_{\rm gr}(\boldsymbol{k}) \right) \cdot \Delta \boldsymbol{q} \right| . \tag{5.82}$$

For resonant packets, this is proportional to the difference of straining wave group and phase speeds, reminiscent of what we encountered in our discussion of quasi-linear theory. This time scale is relevant to 'pure' weak turbulence theory

— with resonance broadening—the self-decorrelation rate of the straining wave or test wave. These are nonlinear timescales related to wave dynamics and enter when resonance broadening is considered. For example, the test wave lifetime is often of the order of magnitude of the inverse growth rate $|\gamma_{\boldsymbol{k}}|$.

Like the parametric subharmonic process, the effect of induced diffusion also is sensitive to the exciton population profile. Thus, for energy density $E = N\omega$, diffusion of N means the net change of the short wave energy is given by

$$\frac{{\rm d}E_{\rm sw}}{{\rm d}t} = \frac{\rm d}{{\rm d}t} \int {\rm d}\boldsymbol{k}\, E(\boldsymbol{k},t) = - \int {\rm d}\boldsymbol{k}\, \frac{{\rm d}\omega}{{\rm d}\boldsymbol{k}} \cdot \mathsf{D} \cdot \frac{{\rm d}N}{{\rm d}\boldsymbol{k}}. \tag{5.83}$$

Hence, the poulation profile gradient ${\rm d}N/{\rm d}\boldsymbol{k}$ and the group velocity ${\rm d}\omega/{\rm d}\boldsymbol{k}$ together determine ${\rm d}E_{\rm sw}/{\rm d}t$. For ${\rm d}\omega/{\rm d}\boldsymbol{k} > 0$, ${\rm d}N/{\rm d}\boldsymbol{k} \lessgtr 0$ implies ${\rm d}E_{\rm sw}/{\rm d}t \gtrless 0$, with correspondingly opposite results for ${\rm d}\boldsymbol{\omega}/{\rm d}\boldsymbol{k} < 0$. Of course, ${\rm d}E_{\rm sw}/{\rm d}t > 0$ means the short waves are *gaining* energy from the straining waves, while ${\rm d}E_{\rm sw}/{\rm d}t < 0$ means that they are *losing* energy to the longer wavelengths.

It is interesting to note that induced diffusion is one limit where the fundamental origin of irreversibility in wave turbulence is rigorously clear. In eikonal theory, $\boldsymbol{k} = \boldsymbol{\nabla}\phi$, where ϕ is the wave phase function. Then,

integrating the eikonal equation for $\boldsymbol{k}$ gives

$$\frac{\mathrm{d}}{\mathrm{d}t}\delta\phi = -\left(\tilde{\omega} + \boldsymbol{k}\cdot\tilde{\boldsymbol{v}}\right), \tag{5.84a}$$

so

$$\left\langle \delta\phi^2 \right\rangle = D_\phi t, \tag{5.84b}$$

where the phase diffusion coefficient is

$$D_\phi = \sum_{\boldsymbol{q}} \left| \left(\tilde{\omega} + \boldsymbol{k}\cdot\tilde{\boldsymbol{v}}\right)_{\boldsymbol{q}} \right|^2 \tau_{\boldsymbol{k},\boldsymbol{q}} \tag{5.85a}$$

and in weak wave turbulence,

$$\tau_{\boldsymbol{k},\boldsymbol{q}} \to \pi\delta\left(\omega_{\boldsymbol{q}} - \boldsymbol{q}\cdot\boldsymbol{v}_{\mathrm{gr}}(\boldsymbol{k})\right). \tag{5.85b}$$

Thus, we see that if resonances between the strain field phase velocity and the wave packet group velocity overlap (in the sense of island overlap, ala Chirikov, the wave phase will evolve diffusively, consistent with the notion of a random phase. Here then, *ray stochasticity*, emerges as the dynamical underpinning of irreversibility for induced diffusion. More generally, since a range of large scale waves or straining flows is an ubiquitous element in fluctuation spectra, it is tempting to speculate that the utility of RPA-based techniques may be rooted in phase stochasticity driven by induced diffusion. This is especially likely when the straining field and the energy containing regions of the spectrum coincide. This speculation could be explored by comparing the coherent energy transfer rate in a resonant triad (i.e. γ_E) with the rate at which the frequency wanders due to phase stochastization by straining during that time period, i.e. $\Delta\omega_{\mathrm{phase}} \sim (v_{\mathrm{gr}}^2 q^2 D_\phi/\gamma_E)^{1/2}$.

5.5.2 Effects of large/meso scale modes on micro fluctuations

Non-local interactions have received far less attention than local, 'Kolmogorov' cascades in wave turbulence. Nevertheless, non-local interactions are of great importance since they:

— are useful as a framework for describing large scale structure formation in turbulence.

— describe and account for interactions which break scale invariance and so induce intermittency.

We now briefly discuss these two important roles of non-local interactions. One frequently utilized approach to the problem of structure formation is to consider when and how an ambient spectrum of waves and turbulence is, in some sense, unstable to the growth of a large scale seed perturbation. For example, in mean field dynamo theory one considers the stability of a spectrum of turbulence to a large scale magnetic field. The induced diffusion interaction, introduced here and developed much further in Chapter 7, is especially useful for this type of consideration, since it naturally describes the exchange of energy between an ambient short wavelength wave spectrum and a seed spectrum of large scale excitations. The theory can be extended to address saturation of structure formation by a variety of processes, including self-consistent alteration or evolution of the ambient wave spectrum. This picture of coupled evolution of the large scale strain field and smaller scale wave field (which exerts a stress on the former) leads naturally to a 'predator-prey' type model of the self-consistent interaction of the two components, as discussed further in Vol. II. Parametric subharmonic decay interaction is also interesting as a means for non-local transfer of energy in frequency

—from a pump to lower frequency waves. This mechanism is exploited in some scenarios of low-frequency structure formation.

Non-local interactions are of interest as a possible origin of intermittency. Of course, intermittency has many forms and many manifestations. One frequently invoked definition of intermittency is that of "a process which breaks scale similarity by inducing an explicit memory of one class of scales in another," the connection of which is driven by a cascade. For example, the β-model and multi-fractal models of inertial range intermittancy in K41 turbulence all invoke a notion of embedded turbulence, where a 'footprint' of the stirring scale l_0 survives in the inertial range via explicit spectral dependence on l_0 (N.B. Here 'explicit' means dependence on (l_0) not only via the dissipation rate ϵ). Non-local interactions clearly can produce such multi-scale memory—random straining (as occurs in induced diffusion) will surely leave an imprint of a large scale, energetic strain field on smaller wave scales. Of course, the size and strength of this effect will to some extent depend upon the relative sizes of the large-scale induced distortion or strain rate and the rate of local energy transfer among smaller scales. In this regard it is worth noting that a recent interesting line of research (Laval et al., 2001) on the dynamics of intermittency in 3D Navier-Stokes turbulence has suggested a picture where:

— like-scale interactions are self-similar and non-intermittent, and are responsible for most of the energy transfer. These are well described by conventional scaling arguments.

— disparate scale straining is the origin of scale symmetry breaking and intermittency, and is well described by Rapid Distortion Theory, which is closely related to induced diffusion.

Apart from its intrinsic interest, this approach to the problem of intermittency is noteworthy since it is entirely compatible with a simple statistical or weak turbulence model, and does not require invoking more exotic theoretical concepts such as multi-fractality, coherent structures, etc.

5.5.3 Induced diffusion equation for internal waves

As a case study in non-local interaction, we focus on the interaction of oceanic internal waves. Internal waves (IW's) have dispersion relation

$$\omega^2 = k_{\mathrm{H}}^2 N_{\mathrm{BV}}^2 / k^2, \tag{5.86a}$$

where N_{BV} is the Brunt-Väisälä (BV) buoyancy frequency, i.e.

$$N_{\mathrm{BV}}^2 = +\frac{g}{\rho_0}\frac{\mathrm{d}\rho_0}{\mathrm{d}z}, \tag{5.86b}$$

where z grows with depth, down from the surface, so IW's may be thought of as the stable counterpart to the Rayleigh-Taylor instability for the case of a continuous density profile (i.e. no interface). Here k_{H} refers to the horizontal wavenumber and k_{V} is the vertical wavenumber, so $k^2 = k_{\mathrm{H}}^2 + k_{\mathrm{V}}^2$. Internal waves are excited at mesoscales by Rossby waves, the interaction of large currents with bottom topography, and large storms. IW interaction generates a broad spectrum of IW's which is ultimately limited by breaking and over-turning at small scales. A phenomenological model of the IW spectrum, called the Garret-Munk (GM) model (Garret and Munk, 1975), provides a reasonable fit to the measured IW spectrum. The GM spectrum density of IW's is peaked at large scales.

In an edifying and broadly relevant study, McComas and Bretherton (McComas and Bretherton, 1977) identified three types of non-local interactions which occur in IW turbulence. There are:

— induced diffusion

— parametric subharmonic instability

— elastic scattering

In all cases, the origin of the generic type of interaction can be traced to the wave dispersion relation structure and the basic wave-wave coupling equations. Here, we outline the key points of this instructive analysis. In this context, the wave population density is denoted by $A(\boldsymbol{k})$ (to avoid confusion with BV frequency N) and the wave-wave collision integral has the generic form following Eq. (5.33), i.e.

$$\begin{aligned}\frac{\mathrm{d}}{\mathrm{d}t}A(\boldsymbol{k}) = F\{A\} = \int \mathrm{d}\boldsymbol{k}' \int \mathrm{d}\boldsymbol{k}'' \big\{ & D^{+}\delta\left(\boldsymbol{k}' + \boldsymbol{k}'' - \boldsymbol{k}\right)\delta\left(\omega' + \omega'' - \omega\right) \\ & \times \left[A(\boldsymbol{k}')A(\boldsymbol{k}'') - A(\boldsymbol{k}')A(\boldsymbol{k}) - A(\boldsymbol{k}'')A(\boldsymbol{k})\right] \\ & + 2D^{-}\delta\left(\boldsymbol{k}' - \boldsymbol{k}'' - \boldsymbol{k}\right)\delta\left(\omega' - \omega'' - \omega\right) \\ & \times \left[A(\boldsymbol{k}')A(\boldsymbol{k}'') + A(\boldsymbol{k}')A(\boldsymbol{k}) - A(\boldsymbol{k}'')A(\boldsymbol{k})\right]\big\}\,.\end{aligned} \tag{5.87}$$

Here D^{+} and D^{-} are coupling coefficients, and the notation is obvious.

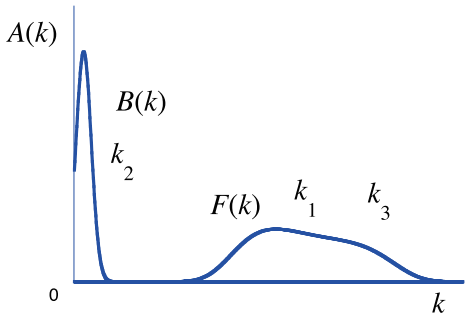

Fig. 5.15. Cartoon of long wave-short wave interactions. The spectral function $A\,(k)$ is composed of $B\,(k)$ and $F\,(k)$.

To extract induced diffusion from $F\{A\}$, it is useful to divide the spectrum into two pieces, as shown in Fig. 5.15. In that cartoon,

— $\boldsymbol{k}_2$ refers to the straining waves at large scale, with spectral density $B(\boldsymbol{k}_2)$
— $\boldsymbol{k}_1$ and $\boldsymbol{k}_3$ are the short wavelength waves, with spectral density $F(\boldsymbol{k}_{1,3})$

Thus,

$$A(\boldsymbol{k}) = B(\boldsymbol{k}) + F(\boldsymbol{k}).$$

We assume B and F do not overlap, so $B(\boldsymbol{k}_3) = B(\boldsymbol{k}_1) = 0$. Since short wavelength evolution due to large scale wave effects is of interest here, we seek $\partial F(\boldsymbol{k}_3)/\partial t$, and can re-write Eq. (5.87) as

$$\begin{aligned}\frac{\partial}{\partial t}F(\boldsymbol{k}_3) = \int \mathrm{d}\boldsymbol{k}' \int \mathrm{d}\boldsymbol{k}'' \big\{ & D^+\delta\left(\boldsymbol{k}' + \boldsymbol{k}'' - \boldsymbol{k}_3\right)\delta\left(\omega' + \omega'' - \omega_3\right) \\ & \times \big[B(\boldsymbol{k}')\left(F(\boldsymbol{k}'') - F(\boldsymbol{k}_3)\right) + B(\boldsymbol{k}'')\left(F(\boldsymbol{k}') - F(\boldsymbol{k}_3)\right) + F(\boldsymbol{k}')F(\boldsymbol{k}'') \\ & -F(\boldsymbol{k}_3)F(\boldsymbol{k}') - F(\boldsymbol{k}_3)F(\boldsymbol{k}'')\big] + 2D^-\delta\left(\boldsymbol{k}' - \boldsymbol{k}'' - \boldsymbol{k}_3\right)\delta\left(\omega' - \omega'' - \omega_3\right) \\ & \times \big[B(\boldsymbol{k}'')\left(F(\boldsymbol{k}') - F(\boldsymbol{k}_3)\right) + F(\boldsymbol{k}_3)F(\boldsymbol{k}') - F(\boldsymbol{k}_3)F(\boldsymbol{k}) - F(\boldsymbol{k}_3)F(\boldsymbol{k}'')\big]\big\}.\end{aligned} \tag{5.88}$$

The point here is to isolate the influence of the large scale waves on the smaller scales. Hence, we decompose $\partial F(\boldsymbol{k}_3)/\partial t$ into

$$\frac{\partial F(\boldsymbol{k}_3)}{\partial t} = \left.\frac{\partial F(\boldsymbol{k}_3)}{\partial t}\right|_{\text{local}} + \left.\frac{\partial F(\boldsymbol{k}_3)}{\partial t}\right|_{\text{non-local}} \tag{5.89a}$$

and can read off $\partial F(\boldsymbol{k}_3)/\partial t|_{\text{non-local}}$ from Eq. (5.88) as

$$\begin{aligned}\left.\frac{\partial}{\partial t}F(\boldsymbol{k}_3)\right|_{\text{non-local}} = 2\int \mathrm{d}\boldsymbol{k}_1 \int \mathrm{d}\boldsymbol{k}_2 \\ \big\{D^+\delta\left(\boldsymbol{k}_1 + \boldsymbol{k}_2 - \boldsymbol{k}_3\right)\delta\left(\omega_1 + \omega_2 - \omega_3\right)B(\boldsymbol{k}_2)\left[F(\boldsymbol{k}_1) - F(\boldsymbol{k}_3)\right] \\ +D^-\delta\left(\boldsymbol{k}_1 - \boldsymbol{k}_2 - \boldsymbol{k}_3\right)\delta\left(\omega_1 - \omega_2 - \omega_3\right)B(\boldsymbol{k}_2)\left[F(\boldsymbol{k}_1) - F(\boldsymbol{k}_3)\right]\big\}.\end{aligned} \tag{5.89b}$$

Here the spectral energy is contained predominantly in $B(\boldsymbol{k}_2)$. Now expanding about $\boldsymbol{k}_3$ in the first term in brackets while expanding about $\boldsymbol{k}_1$ in the

second term in brackets, and noting that D^+ and D^- are real and symmetric in indices give

$$\begin{aligned}
&\frac{\partial}{\partial t}F(\boldsymbol{k}_3)\bigg|_{\text{non-local}} = \\
&\quad = 2\int \mathrm{d}\boldsymbol{k}_1 \int \mathrm{d}\boldsymbol{k}_2 \, \{\delta\left(\boldsymbol{k}_1+\boldsymbol{k}_2-\boldsymbol{k}_3\right)\delta\left(\omega\left(\boldsymbol{k}_3+\left(\boldsymbol{k}_2-\boldsymbol{k}_3\right)\right)+\omega(\boldsymbol{k}_3)+\omega(\boldsymbol{k}_2)\right) \\
&\qquad \times B(\boldsymbol{k}_2)\left[F\left(\boldsymbol{k}_3+\left(\boldsymbol{k}_1-\boldsymbol{k}_3\right)\right)-F(\boldsymbol{k}_3)\right] \\
&\quad + 2\int \mathrm{d}\boldsymbol{k}_1 \int \mathrm{d}\boldsymbol{k}_2 \, \{\delta\left(\boldsymbol{k}_1-\boldsymbol{k}_2-\boldsymbol{k}_3\right)\delta\left(\omega(\boldsymbol{k}_1)-\omega(\boldsymbol{k}_2)-\omega\left(\boldsymbol{k}_1+\left(\boldsymbol{k}_3-\boldsymbol{k}_1\right)\right)\right) \\
&\qquad \times B(\boldsymbol{k}_2)\left[F(\boldsymbol{k}_1)-F\left(\boldsymbol{k}_3+\left(\boldsymbol{k}_1-\boldsymbol{k}_3\right)\right)\right] \\
&\quad = 2\int \mathrm{d}\boldsymbol{k}_1 \int \mathrm{d}\boldsymbol{k}_2 \, H(\boldsymbol{k})B(\boldsymbol{k}_2)\left(\boldsymbol{k}_1-\boldsymbol{k}_3\right)\cdot\left[\frac{\partial}{\partial\boldsymbol{k}}F(\boldsymbol{k}_1)-\frac{\partial}{\partial\boldsymbol{k}}F(\boldsymbol{k}_3)\right],
\end{aligned} \tag{5.89c}$$

where

$$H(\boldsymbol{k}) = D^+\delta\left(\boldsymbol{k}_1+\boldsymbol{k}_2-\boldsymbol{k}_3\right)\delta\left(\omega_1+\omega_2-\omega_3\right). \tag{5.89d}$$

Again expanding about $\boldsymbol{k}_3$ finally yields

$$\frac{\partial}{\partial t}F(\boldsymbol{k}_3) = \frac{\partial}{\partial\boldsymbol{k}_3}\cdot\mathsf{D}_{\boldsymbol{k}}\cdot\frac{\partial}{\partial\boldsymbol{k}_3}F(\boldsymbol{k}_3). \tag{5.90a}$$

Here the $\boldsymbol{k}$-space diffusion tensor $\mathsf{D}_{\boldsymbol{k}}$ is given by

$$\begin{aligned}
\mathsf{D}_{\boldsymbol{k}} =& 2\int \mathrm{d}\boldsymbol{k}_1 \int \mathrm{d}\boldsymbol{k}_2 \, D^+B(\boldsymbol{k}_2) \\
&\times\left[\left(\boldsymbol{k}_3-\boldsymbol{k}_1\right)\left(\boldsymbol{k}_3-\boldsymbol{k}_1\right)\right]\delta\left(\boldsymbol{k}_1+\boldsymbol{k}_2-\boldsymbol{k}_3\right)\delta\left(\omega_2-\boldsymbol{k}_2\cdot\boldsymbol{v}_{\mathrm{gr}}(\boldsymbol{k}_3)\right),
\end{aligned} \tag{5.90b}$$

and the same procedure as in Eqs. (5.81a), (5.81b) has been used to simplify the frequency matching condition.

The brief calculation sketched above shows that induced diffusion can be recovered from a systematic expansion of $C\{N\}$, and so is more robust than suggested by the heuristic, back-of-the-envelope argument using the eikonal equations. Clearly, induced diffusion corresponds to adiabatic modulation

of short waves by long ones, and so should conserve the total number of wave quanta, as required by the Manley-Rowe relations (Eq. (5.13)). Equation (5.89) clearly *does* satisfy quanta conservation. In view of its foundation in adiabatic theory, it is not surprising then, that induced diffusion can also be derived from mean field theory for the collisionless wave kinetic equation. Treating the refractive term as multiplicative modulation induced by large scale perturbations, and neglecting $C\{N\}$, the wave kinetic equation is

$$\frac{\partial N}{\partial t} + v_{\mathrm{gr}} \cdot \boldsymbol{\nabla} N - \frac{\partial}{\partial \boldsymbol{x}} \left(\tilde{\omega} + \boldsymbol{k} \cdot \tilde{\boldsymbol{v}}\right) \cdot \frac{\partial N}{\partial \boldsymbol{k}} = 0, \tag{5.91a}$$

so the mean field equation for a spatially homogeneous (or slowly varying) mean population $\langle N \rangle$ is

$$\frac{\partial \langle N \rangle}{\partial t} = \frac{\partial}{\partial \boldsymbol{k}} \cdot \left\langle \left(\frac{\partial}{\partial \boldsymbol{x}} \left(\tilde{\omega} + \boldsymbol{k} \cdot \tilde{\boldsymbol{v}}\right) \right) \tilde{N} \right\rangle. \tag{5.91b}$$

Then, writing

$$\begin{pmatrix} \tilde{\omega} \\ \tilde{\boldsymbol{v}} \end{pmatrix} = \sum_{\boldsymbol{q},\Omega} \begin{pmatrix} \tilde{\omega}_{\boldsymbol{q}} \\ \tilde{\boldsymbol{v}}_{\boldsymbol{q}} \end{pmatrix} \exp\left(i\left(\boldsymbol{q} \cdot \boldsymbol{x} - \Omega t\right)\right), \tag{5.91c}$$

where $|\boldsymbol{q}| \ll |\boldsymbol{k}|$ and $\Omega \ll \omega$ and computing the linear response $\tilde{N}$ of the population to the modulation field gives

$$\tilde{N}_{\boldsymbol{q},\Omega} = \frac{-\boldsymbol{q}\left(\tilde{\omega} + \boldsymbol{k} \cdot \tilde{\boldsymbol{v}}\right)_{\boldsymbol{q},\Omega}}{\left(\Omega - \boldsymbol{q} \cdot \boldsymbol{v}_{\mathrm{gr}}\right)} \cdot \frac{\partial \langle N \rangle}{\partial \boldsymbol{k}}. \tag{5.92}$$

A simple quasilinear closure of Eq. (5.91b) finally gives the induced diffusion equation

$$\frac{\partial \langle N \rangle}{\partial \boldsymbol{k}} = \frac{\partial}{\partial \boldsymbol{k}} \cdot \mathsf{D}_{\boldsymbol{k}} \cdot \frac{\partial \langle N \rangle}{\partial \boldsymbol{k}}, \tag{5.93a}$$

where the diffusion tensor is

$$\mathsf{D}_{\boldsymbol{k}} = \sum_{\boldsymbol{q}} \boldsymbol{q}\boldsymbol{q} \left| \left(\tilde{\omega} + \boldsymbol{k} \cdot \tilde{\boldsymbol{v}}\right)_{\boldsymbol{q}} \right|^2 \pi \delta\left(\Omega - \boldsymbol{q} \cdot v_{\mathrm{gr}}(\boldsymbol{k})\right). \tag{5.93b}$$

The correspondence between Eq. (5.93b) and Eq. (5.90b) is obvious. Induced diffusion and its role in the self-consistent description of disparate scale interaction processes will be discussed in much more depth in Chapter 7 and in Volume II.

5.5.4 Parametric interactions revisited

Parametric subharmonic interaction is best approached first from the viewpoint of coherent interaction, and then subsequently discussed in the context of wave kinetics. At its roots, parametric-subharmonic interaction occurs due to parametric variation in wave oscillation frequency. Thus for linear internal waves (IWs), where $\omega^2 = k_{\mathrm{H}}^2 N_{\mathrm{BV}}^2/k^2$, a fluid element will oscillate vertically according to

$$\frac{\mathrm{d}^2 z}{\mathrm{d}t^2} + \frac{k_{\mathrm{H}}^2}{k^2} N_{\mathrm{BV}}^2 z = 0.$$

If parametric variation is induced in the BV frequency (Eq. (5.86b)) at some frequency Ω, so N_{BV}^2 becomes time-dependent, i.e.

$$N_{\mathrm{BV}}^2 = \frac{k_{\mathrm{H}}^2}{k^2} N_{\mathrm{BV},0}^2 \left(1 + \delta \cos\left(\Omega t\right)\right),$$

then the motion of the fluid element may exhibit *parametric growth* according to the solution of the Mathieu equation

$$\frac{\mathrm{d}^2 z}{\mathrm{d}t^2} + \frac{k_{\mathrm{H}}^2}{k^2} N_{\mathrm{BV},0}^2 \left(1 + \delta \cos\left(\Omega t\right)\right) z = 0.$$

In particular, it is well known that parametric instability will occur for $\Omega \sim 2\omega_{\mathrm{IW}} \sim 2\left(k_{\mathrm{H}}^2 N_{\mathrm{BV},0}^2/k^2\right)^{1/2}$. Of course, this simple argument completely ignores spatial dependence. In the context of IW's (or any other waves), *both* wave-number and frequency matching conditions must be satisfied, so

that

$$\boldsymbol{k}_3 = \boldsymbol{k}_1 + \boldsymbol{k}_2,$$

$$\omega_3 = \omega_1 + \omega_2.$$

Now, it is interesting to observe that one can 'arrange' a high-frequency, but spatially quasi-homogeneous variation in the BV frequency by a three-wave interaction where $\boldsymbol{k}_1 = -\boldsymbol{k}_2 + \epsilon\boldsymbol{k}$ (here $\epsilon \ll 1$) and $\omega_1 \sim \omega_2$. For this pair of counter-propagating waves with comparable frequencies, we have $\boldsymbol{k}_3 = \boldsymbol{k}_1 + \boldsymbol{k}_2 = \epsilon\boldsymbol{k}$ and $\omega_3 \sim 2\omega$, which is precisely the sought after situation of spatially uniform parametric variation. Of course, coherent resonant three-wave interactions are reversible, so we can view this traid as one consisting of:

— a 'pump,' at $\omega_3 \sim 2\omega$, with $|\boldsymbol{k}_3| \sim O(\epsilon)$
— two 'daughter' waves at $\boldsymbol{k}_1$, ω_1 and $\boldsymbol{k}_2 = -\boldsymbol{k}_1 + \epsilon\boldsymbol{k}$, ω_1.

In this light, we easily recognize the parametric-subharmonic instability as a variant of the decay instability, discussed earlier in Section 5.2 of this chapter. Thus, taking $a_3 \sim$ const. as the pump, Eqs. (5.16) immediately can be applied, so (noting that here, the coupling coefficient is D),

$$i\omega\frac{\mathrm{d}a_1}{\mathrm{d}t} = Da_2^* a_3, \tag{5.94a}$$

$$i\omega\frac{\mathrm{d}a_2}{\mathrm{d}t} = Da_1^* a_3, \tag{5.94b}$$

so the parametric-subharmonic growth rate is just:

$$\gamma_{\mathrm{PS}}^2 = \frac{D^2}{\omega^2}\left|a_3\right|^2. \tag{5.94c}$$

To see how parametric-subharmonic instability emerges in wave kinetics, it is convenient to take $\boldsymbol{k}_2$ as the pump, so $A(\boldsymbol{k}_2) \gg A(\boldsymbol{k}_1), A(\boldsymbol{k}_3)$, and

$|\boldsymbol{k}_2| \ll |\boldsymbol{k}_1|, |\boldsymbol{k}_3|$, $\omega_2 \approx 2\omega_1$. In this limit, we can neglect contributions to the wave kinetic equation for $A(\boldsymbol{k}_2)$, which are proportional to the product $A(\boldsymbol{k}_1)A(\boldsymbol{k}_2)$, just as we neglected terms of $O(a_1, a_2)$ in the coherent equations. This gives

$$\frac{\partial A(\boldsymbol{k}_2)}{\partial t} \cong -\int \mathrm{d}\boldsymbol{k}_1 \int \mathrm{d}\boldsymbol{k}_3 \, D\delta\left(\boldsymbol{k}_1 + \boldsymbol{k}_3 - \boldsymbol{k}_2\right) \delta\left(\omega_1 + \omega_3 - \omega_2\right) \times \left[\left(A(\boldsymbol{k}_1) + A(\boldsymbol{k}_3)\right) A(\boldsymbol{k}_2)\right], \tag{5.95}$$

which describes the depletion in the pump energy due to parametric-subharmonic coupling to $\boldsymbol{k}_1$ and $\boldsymbol{k}_3$. Related expressions for the growth of $A(\boldsymbol{k}_1)$ and $A(\boldsymbol{k}_3)$ are easily obtained from the general expression for $C\{A\}$, given in Eq. (5.87). Energy transfer by parametric-subharmonic interaction will continue until the pump is depleted, i.e. until $A(\boldsymbol{k}_2) \sim A(\boldsymbol{k}_1), A(\boldsymbol{k}_3)$. Equation (5.95) is also consistent with our earlier observation concerning the ratio of the growth rates for stochastic and coherent decay processes. Once again, for parametric-subharmonic (PS) interaction, we have $\gamma_{\mathrm{PS}}^{\mathrm{stoch}}/\gamma_{\mathrm{PS}}^{\mathrm{coh}} \sim \tau_{T_c}\gamma_E^{\mathrm{coh}}$. Thus in wave kinetics, the interaction growth is reduced in proportion to the ratio of the triad coherence time to the coherent growth rate interaction.

Induced diffusion and parametric-subharmonic interaction both involve the interaction of nearly counter-propagating waves with a low $\boldsymbol{k}$ wave. In one case (induced diffusion), the frequencies nearly cancel too, while in the other (parametric-subharmonic) the frequencies add. These triads are shown in Fig. 5.16. The third type of non-local interaction, called *elastic scattering*, is complementary to the other two, in that the magnitudes of the interacting $\boldsymbol{k}$'s are *comparable* and only the frequencies are *disparate*. For elastic scattering, we consider a triad of $\boldsymbol{k}_1$, $\boldsymbol{k}_2$, $\boldsymbol{k}_3$ with

— $k_{1\mathrm{H}} \sim k_{3\mathrm{H}}$, $k_{1,\mathrm{V}} \sim -k_{3,\mathrm{V}}$ with $k_{1,\mathrm{V}} < 0$

— $k_{\mathrm{V}_1} \sim 2k_{\mathrm{V}_2}$, so $k_{\mathrm{V}_1} + k_{\mathrm{V}_2} = k_{\mathrm{V}_3}$

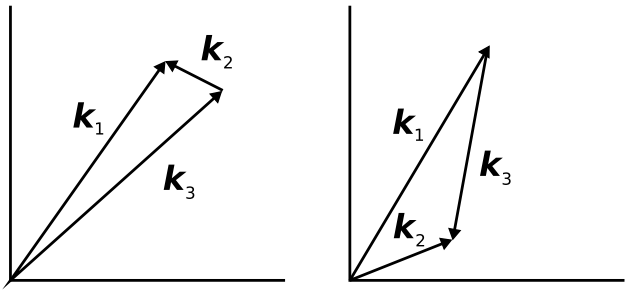

(a) Induced Diffusion:
— $\boldsymbol{k}_1$, $\boldsymbol{k}_3$ nearly *parallel*
— difference beat at *low* frequency

(b) Parametric-Subharmonic:
— $\boldsymbol{k}_1$, $\boldsymbol{k}_3$ nearly *opposite*
— pump = *sum* beat at *high* frequency

Fig. 5.16. Triad structure for non-local interactions of induced diffusion, parametric subharmonic types.

— $\omega_2 < \omega_1, \omega_3$.

The coherent interaction equations for the amplitudes c_1, c_2, c_3 are

$$i\omega \frac{\mathrm{d}c_1}{\mathrm{d}t} = Dc_2^* c_3, \tag{5.96a}$$

$$i\omega \frac{\mathrm{d}c_2}{\mathrm{d}t} = Dc_1^* c_3, \tag{5.96b}$$

$$i\omega \frac{\mathrm{d}c_3}{\mathrm{d}t} = Dc_1 c_2, \tag{5.96c}$$

so the energies $E_i = \omega_i^2 \left|c_i\right|^2$, $i = 1, 2, 3$ evolve according to

$$\frac{\partial E_1}{\partial t} = -\omega_1 R, \tag{5.97a}$$

$$\frac{\partial E_2}{\partial t} = \omega_2 R, \tag{5.97b}$$

$$\frac{\partial E_3}{\partial t} = \omega_3 R, \tag{5.97c}$$

where $R = -D\,\mathrm{Im}\,\{c_1^* c_2^* c_3\}$. Since $\omega_2 \ll \omega_1, \omega_3$, E_2 is nearly constant, as compared to E_1 and E_3, so the essential dynamics are described by Eqs. (5.97a), (5.97c), i.e.

$$\frac{\partial E_1}{\partial t} = -\omega_1 R \quad ; \quad \frac{\partial E_3}{\partial t} = \omega_3 R.$$

Thus, we see that in this system, energy is exchanged between modes 1 and 3, moving through the static, low-frequency field of mode 2. The low-frequency scattering field is essentially unaffected by the scattering process—hence the name "elastic scattering." As in the familiar case of Bragg scattering, waves 1 and 3 are back-scattered by the component of the background with half the vertical wavelength of the scattered wave. Elastic scattering is instructive, as it illustrates the rich variety of non-local interactions possible among nonlinearly interacting dispersive waves in anisotropic media. The types of non-local interactions at work in internal wave turbulence are summarized in Table 5.3.

Some advanced topics in wave interactions such as the weak turbulence of filamentary structures (Dyachenko et al., 1992) and limited domains of resonance overlap (Kartashova, 2007) are discussed in the research literatures.

Table 5.3. *Summary of non-local internal wave interactions*

i.) **Induced Diffusion**

— $\begin{cases} \Omega_2 \sim \omega_1 - \omega_3 \ll \omega_1, \omega_3 \\ |\boldsymbol{k}_2| \sim |\boldsymbol{k}_1 - \boldsymbol{k}_3| \ll |\boldsymbol{k}_1, \boldsymbol{k}_3| \end{cases}$

— slow, stochastic straining by low frequency, large scale

— diffusion in $\boldsymbol{k}$

ii.) **Parametric-Subharmonic Interaction**

— $\begin{cases} \Omega_2 \sim \omega_1 + \omega_3 > \omega_1, \omega_3 \\ |\boldsymbol{k}_2| \sim |\boldsymbol{k}_1 + \boldsymbol{k}_3| < |\boldsymbol{k}_1|, |\boldsymbol{k}_3| \end{cases}$

— pumping by high frequency

— decay instability

iii.) **Elastic Scattering**

— $\begin{cases} |\boldsymbol{k}_1| \sim |\boldsymbol{k}_2| \sim |\boldsymbol{k}_3| \\ \omega_2 < \omega_1, \omega_3 \end{cases}$

— wave packets 1, 3 on static scattering field of 2

— elastic scattering, ala Bragg